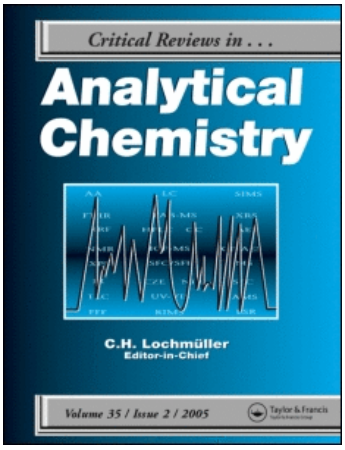

Critical Reviews in Analytical Chemistry
Publication details, including instructions for authors and subscription information:
http://www.informaworld.com/smpp/title~content=t713400837

Mixed-Gas, Molecular-Gas, and Helium Inductively Coupled Plasmas for Analytical Atomic Spectrometry: A Critical Review

Akbar Montaser; Raymond L. Van Hoven; Ramon M. Barnes

To cite this Article Montaser, Akbar , Van Hoven, Raymond L. and Barnes, Ramon M.(1987) 'Mixed-Gas, Molecular-Gas, and Helium Inductively Coupled Plasmas for Analytical Atomic Spectrometry: A Critical Review', Critical Reviews in Analytical Chemistry, 18: 1, 45 — 103
To link to this Article: DOI: 10.1080/10408348708542801
URL: http://dx.doi.org/10.1080/10408348708542801

MIXED-GAS, MOLECULAR-GAS, AND HELIUM INDUCTIVELY COUPLED PLASMAS FOR ANALYTICAL ATOMIC SPECTROMETRY: A CRITICAL REVIEW

Authors: Akbar Montaser*
Raymond L. Van Hoven
Department of Chemistry
George Washington University
Washington, D.C.

Referee: Ramon M. Barnes
Department of Chemistry
University of Massachusetts
Amherst, Massachusetts

TABLE OF CONTENTS

* Corresponding author.

I. INTRODUCTION

Inductively coupled plasmas (ICPs) operated at atmospheric pressure are commonly used as vaporization-atomization-excitation-ionization sources in analytical atomic emission spectrometry (AES), atomic fluorescence spectrometry (AFS), and mass spectrometry (MS). Argon-supported ICP discharges exhibit several advantages for spectrochemical analysis. They provide high powers of detection and wide concentration dynamic ranges, with minimal matrix effects, and they are extremely useful for simultaneous multielement determinations. Because of ease of operation and a power requirement lower than that for other support gases such as air, nitrogen, oxygen, and hydrogen, most laboratory ICP discharges are sustained in pure argon. This relative ease of operation and reduced power requirement are partly attributed to lower thermal conductivity, lower heat capacity, and lower electrical resistivity of Ar, compared to other support gases.

The first atmospheric pressure ICP discharge, generated with a torch resembling the present configuration, was reported by Reed in 1961.[1] Typical gas flow and rf power requirement were 10 to 20 *l*/min and 1 to 10 kW, respectively. Plasma formation at atmospheric pressure was observed to be easiest in a flowing stream of Ar, but once the discharge was formed, Ar gas mixtures containing 20% air, helium or hydrogen, or 50% oxygen could also be used. In a subsequent publication,[2] Reed reported that diatomic gases and helium were more effective for growing highly refractory crystals because they provide higher heat transfer than Ar. Stimulated by Reed's work, Greenfield and co-workers[3] and Wendt and Fassel[4] were the first investigators to utilize an ICP for analytical atomic emission spectrometry (AES). Subsequent studies[5-8] documented the superior analytical capabilities of the ICP discharges compared to combustion flames and other spectrochemical sources. Based on the number of publications and the greater availability of commercial instrumentation, the ICP-AES is currently more popular than the ICP-MS and the ICP-AFS, a situation that is anticipated to change in the next decade. Relatedly, ICP-atomic absorption spectrometry (AAS) was investigated[9] in the mid-1960s, but its application has been limited to diagnostic studies.[10] The limitations of ICP discharges as atom cells for AAS have been discussed elsewhere.[10] This review article focuses chiefly on AES studies.

The choice of Ar support gas for ICP spectrometry poses several limitations. From an analytical viewpoint, the exciting species in an Ar ICP discharge do not possess sufficient energies to promote electronic transitions in atomic and ionic levels of high excitation energies, such as those of the halogens. Relatedly, certain elements such as sulfur and phosphorus, possessing useful spectral lines in the near UV-visible region,

are subject to spectral interferences by Ar lines.[11,12] Thus, a high-resolution vacuum monochromator, with a purged optical path, is required to observe alternative lines in the vacuum UV region. Alternatively, if nonresonance lines in the near IR region are used, the complex background spectrum of the Ar ICP discharge limits selection of suitable lines for determinations of certain elements, especially the nonmetals.[13] In general, the Ar ICP discharge possesses a structured background above 350 nm and the detection limits of elements with sensitive lines in this spectral region are not sufficiently low for many determinations. From economical consideration, argon is more expensive compared to air, nitrogen, and oxygen, thereby increasing the operating costs of an ICP facility, especially in countries where the argon gas is not produced locally. To reduce the Ar gas requirement, the uses of various low-gas-flow torches have been investigated, and at least three commercial versions of these torches have recently been introduced into the marketplace by Applied Research Laboratories, Labtest Equipment Company, and Sheritt Gordon Mines, Ltd. Although the use of low-gas-flow torches has resulted in a significant reduction of Ar gas-flow requirements, no improvements in the detection powers of the corresponding plasmas have been realized; in certain cases, detection limits measured at spectral lines occurring at wavelengths less than 250 nm have been inferior to those of a conventional Ar ICP discharge.[14]

The above analytical and economic limitations for Ar ICP discharges have been a stimulus for many investigations of mixed gas, molecular gas, and helium ICP discharges. The major impact of mixed-gas and molecular-gas ICPs is their superior ability to decompose refractory particles and to operate with higher solvent and analyte loading compared to Ar ICP, thus extending the domain of samples which could be handled effectively in practice. Also, mixed-gas plasmas are useful tools for elucidating energy transfer mechanisms responsible for suprathermal ionization in pure Ar plasmas[15-18] and for examining physical and transport properties of rf discharges.[19] Both the mixed-gas and molecular-gas ICP discharges possess excellent potentials for the direct analysis of solids[20-26] and for process control.[27] The Baird Corporation has recently introduced an air-ICP atomic emission spectrometer which is chiefly being marketed for process control. As we shall discuss in Section IV, He ICP discharges are especially beneficial for exciting high-excitation energy lines that are either not intense or not observed in the Ar ICP discharges.

This review article addresses the various aspects of analytical ICP discharges operated at atmospheric pressure in gases other than Ar. A summary of previous work on mixed-gas, molecular-gas and helium ICP discharges is given in Section II, along with a description of the formation of the discharges and their physical appearance. The spectral features of the ICP discharges are summarized in Section III. Analytical capabilities of various plasmas in terms of signal-to-background ratios (S/B), detection limits, linear dynamic range, precision, accuracy, and relative freedom from interferences are summarized in Section IV, followed by a list of analytical applications of nonargon ICP discharges. A discussion of discharge characteristics such as electron number density and various temperatures is presented in Section V along with an overview of the computer modeling of related discharges. Future directions for further research and development in this area are also summarized at the conclusion of this survey.

II. FORMATION AND PHYSICAL APPEARANCE OF MIXED-GAS, MOLECULAR-GAS, AND HELIUM ICP DISCHARGES

A. General Trends

The lists of equipment and operating conditions used for generating ICP discharges

with a variety of gases[3,6,13,15-77] are given in Tables 1 to 4. For comparison, the operating conditions commonly used for Ar plasmas[3,28] are listed in Columns 2 and 3 of Table 1 for the Greenfield and Fassel torches, respectively. In almost all studies of mixed-gas plasmas, molecular gases are introduced into either the injector (Table 1), or the outer gas flow (Table 2), of an Ar ICP discharge. Thus, the Ar-H_2S plasma, formed by introducing H_2S into the intermediate gas flow,[78] is not included in these tables.

Four common features are noted when diatomic gases are introduced into the plasma: (1) Mixed-gas or molecular-gas ICP discharges cannot usually be formed directly; rather, molecular gases should be introduced into various flows of an Ar plasma. The transition from pure Ar to a mixed-gas or a molecular-gas ICP discharge takes less than 30 sec. (2) Plasma formation with mixed gas or molecular gases is facilitated significantly if an automatching network is utilized with the crystal-controlled generator. (3) Mixed-gas and molecular-gas plasmas are usually more intense than an Ar ICP operated at the same power. Relatedly, mixed-gas and molecular-gas ICP discharges possess smaller, apparent, luminous volumes compared to the Ar plasma, probably because radiative losses by oxygen, nitrogen, and air, at, for example, 5000 K, are less than that for argon. Despite the smaller apparent volume, gases are very hot in the outer region of the related discharges, and, as discussed in Section V, temperatures of around 5000 K have been measured at the edges of molecular-gas ICP discharges. (4) Compared with operation in pure Ar, higher forward powers and higher gas flows are usually required to stabilize and operate both mixed-gas and molecular-gas ICP discharges. Other specific details regarding introduction of gases in the various gas flows of an ICP discharge are discussed in the following section.

B. Gases in the Injector Flow

Nitrogen,[29-31,33,37,57,59,61,79] oxygen,[29-31,33,36] hydrogen,[34,35,80,81] air,[26,29,31] helium,[30,31] and gases[32,82] such as methane, sulfur dioxide, hydrogen sulfide, sulfur hexafluoride, bromine, and phosphorus trichloride have been introduced into the injector flow of an Ar-supported ICP discharge (Table 1). To stabilize the plasma in a Fassel-type torch, the position of the torch relative to the load coil was raised by about 2 mm and an intermediate gas flow of up to 2.5 *l*/min of Ar was maintained with injector gases such as nitrogen,[57] hydrogen,[34] oxygen,[36] and air.[26] The injector orifice diameter in the torch and the distance between the injector and the base of the discharge were important when pure nitrogen was used by Abdallah and Mermet.[33] Relatedly, the required power increased from 1.3 to 1.6 kW when the Ar injector gas was replaced by nitrogen at a flow rate of 1 *l*/min.[33] Similar observations were noted by others.[30,37,57,61]

Only a few publications[30,57] have addressed the effects of operating conditions on the physical appearance of the plasma. Montaser et al.[57] and Choot and Horlick[61,62] noted that as the percent nitrogen was increased in the injector flow, the axial channel became wider and the plasma length diminished, as shown in Figure 1a, b, and c, while outer diameter of the toroid remained unchanged. Presumably, a portion of energy in the vicinity of the axial channel is used to dissociate the diatomic injector gas, thus reducing the temperature of the axial channel. In fact, the poor plasma-sample interaction[57,61,62] has been attributed to the thin plasma toroid.

C. Gases in the Outer Flow

Visual observations of ICP discharges indicate that the diameter of the axial channel and the apparent, luminous volume of the plasma are reduced when diatomic gases

Table 1
EQUIPMENT AND OPERATING CONDITIONS USED FOR ICPs OPERATED WITH MOLECULAR GASES AND HELIUM IN THE INJECTOR FLOW

References	3	28	29	30, 31	32	33	26	34, 35	36, 37
Equipment									
Generator model	Radyne S.C.15	Plasma-Therm 2500 D	Radyne	Lepel T-5-3-MC-J-B	STEL 5060	R.C. Durr	Lepel T-10-3-MC1-X-SA	Plasma-Therm 2500	Plasma-Therm 2500
Generator type[a]	f.r.	c.c.	f.r.	u.s.[c]	u.s.	u.s.	c.c.	c.c.	c.c.
Frequency, MHz	36.0	27.0	6.0	8.0	5.4	40.0	27.0	27.0	27.0
Torch type[b]	G	F	G	Torch of Reference 4 with exterior outer tube	Demountable	Demountable	Modified F	F	F
Nominal power, kW	2.5	2.5	2.5	5.0	6.0	4.0	10.0	1.5	2.5
Operating conditions									
Forward power, kW	2.5	1.1	2.5	0.7—2.5	6.0	1.3—1.6	1.5	0.7—1.0	1.5—2.0
Observation height, mm	10.0—18.0	12.0—18.0	10.0—18.0	u.s.	0—12.0	5.0	10.0	9.0—14.0	—
Outer gas flow, *l*/min Ar	17 Ar	20 Ar	10—33 Ar	16—18 Ar	7—22 Ar	0	18 Ar	10 Ar	13 Ar
Intermediate gas flow, *l*/min Ar	5 Ar	0 Ar	23—43 Ar	0.4—0.5 Ar	7 Ar	12 Ar	0.6 Ar	0—0.3 Ar	0—2 Ar
Injector gas flow and type, *l*/min	5.0 Ar	1.0 Ar	5.0 Ar, N_2, O_2 or air	O_2, N_2, air, Ar, He	1.5 as: 10% CH_4, SO_2, in 90% Ar	1.0 as: 75% Ar and 25% N_2 or O_2	0.96 air	0—0.7, 6.5% H_2 in 93.5% Ar	0.5 Ar + 0.25 O_2 or 0.65 Ar + 0.07 N_2
Plasma configuration	Annular	Annular	Annular	Ellipsoid	Annular	Annular	Annular	Annular	Annular

[a] f.r., free running generator; c.c., crystal controlled generator.
[b] G, Greenfield torch; F, Fassel torch.
[c] u.s., unspecified.

Table 2
EQUIPMENT AND OPERATING CONDITIONS USED FOR ICPs OPERATED WITH VARIOUS MOLECULAR GASES IN THE OUTER FLOW

References	29	6[a]	30[a]	44[a]	25	46	47[d]	50	51[a]	55	56	23[f]	57[a]	34, 35	17	13[a]	65, 66
Equipment																	
Generator model	Radyne	Radyne RD 150/H	Lepel T-5-3-MC-J-B	PH 1412/10	Linn FS-10	Linn FS-10	Radyne R50P	Radyne R50P	Linn FS-4	Linn FS-4	Linn FS-4	Radyne S.C. 15	Plasma-Therm 5000 D	Plasma Therm	R.C. Durr	Plasma-Therm 2500 D	Modified GP-3.5
Generator type[e]	f.r.[f]	f.r.	u.s.[g]	f.r.	f.r.	f.r.	f.r.	f.r.	f.r.	f.r.	f.r.	f.r.	c.c.[f]	c.c.	t.l.o.[f]	c.c.	c.c.
Frequency, MHz	6.0	7.0	8.0	9.0	27.0	27.0	27.0	27	27.0	27.0	27.0	36.0	27.0	27.0	40.0	27.0	35.0
Torch type[a,b]	G[h]	G	Torch of Reference 4 with exterior outer tube	G	G	G	G	Modified G	G	G	G	G	F[h]	F	Demountable	F	Low-gas flow
Nominal power, kW	2.5	15.0	5.0	12.0	10.0	10.0	5.0	5	4.5	4.5	4.5	2.5	2.5—5.0	1.5	6.0	2.5	5.0
Operating conditions																	
Forward power, kW	u.s.[g]	10.5	0.7—2.5	6.0—12.0	3.0	10.0	5.5	1.2	1.5—3.0	2.8	3.0	2.5	1.0—4.0	0.7—1.0	1.5	1.5—2.3	1.2
Observation height, mm	17.0	10.0—18.0	u.s.	7.0—41.0	4.0—8.0	4.0—8.0	8.0—15.0	10.0—30.0	8.0	8.0	8.0	10.0—18.0	5.0—40.0	9.0—14.0	2.0	2.0—20.0	9.0—13.0
Outer gas flow and type, *l*/min	10—33 Ar, He, and 20% O_2 or N_2 in 80% Ar	20—70 N_2	O_2, N_2, air, Ar, or He	50 Ar, N_2, or air	25 N_2	25 N_2	20 N_2	2—12 N_2	18—27 N_2	16 N_2 or O_2	28 air	7.5 N_2	15—50 0—100% N_2, 100—0% Ar	9 Ar + 1 as 6.5% H_2 in 93.5% Ar	0	15, 0 to 100% N_2 or O_2 or air or 0 to 70% He in Ar	5—7 N_2
Intermediate gas flow, *l*/min	23—43 Ar	4—35 Ar	0.4—0.5 Ar	16 Ar	8 Ar	6 Ar	7.9 Ar	6—12 Ar	11—18 Ar	9 Ar	15 Ar	7.5 Ar	1.5—2.5 Ar	0.3, as 6.5% H_2 in 93.5% Ar	12.5, 0.3% H_2 in Ar	0.2—1.0 Ar	2.5 Ar
Injector gas flow, *l*/min	5.0 Ar	1.5—3.0 Ar	0.4—0.8 Ar	1.5 Ar	1.7 Ar	0.4 Ar	2.0 Ar	0.4 Ar	0.7—1.0 Ar	0.3—0.4 Ar	1.0 Ar	0.5 Ar	1.0—2.5 Ar	0.4, as 6.5% H_2 in 93.5% Ar	1.0—2.0 Ar	0.4—1.5 Ar	0.8—1.5 Ar
Plasma configuration	Annular	Annular	Ellipsoid	Annular	Annular	Annular	Annular	Annular	Annular	Annular	Annular	Annular	Annular	Annular	Annular	Annular	Annular

[a-d] Refers to references with similar equipment and operating conditions: a, 38—43; b, 31; c, 45; d, 48, 49; e, 52—54; f, 40, 41; g, 16,58—60; h, 18, 61—64.

[e] f.r. = free running generator, c.c. = crystal-controlled generator, and t.l.o. = tuned-line oscillator.

[f] G = Greenfield torch, and F = Fassel torch.

[g] u.s. = unspecified.

Table 3
EQUIPMENT AND OPERATING CONDITIONS USED FOR ICPs OPERATED IN PURE MOLECULAR GASES

References	67	68	69	26, 70, 71	27	72
Equipment						
Generator model	Plasma Therm 5000 D	ICP 5000 D	Plasma-Therm MD1 HF15000D	Lepel T-10-3-MCl-X-5-SA	RF Plasma Products 5000D	RF Plasma Product 5000D
Generator type[a]	c.c.	c.c.	c.c.	c.c.	c.c.	c.c.
Frequency, MHz	41.0	41.0	41.0	27.0	41.0	41.0
Torch type[b]	F	Demountable with 18 mm I.D. outer tube	Demountable with 18 mm I.D. outer tube	Demountable with 18 mm I.D. outer tube	MAK	F
Nominal power, kW	5.0	5.0	5.0	10.0	5.0	5.0
Operating conditions						
Forward power, kW	1.3	1.5—2.0	1.5	3.5—3.6	2.2	2.0
Observation height, mm	5.0	0—15.0	u.s.[c]	0—10.0	5.0—15.0	−15 to +40
Gas type	Nitrogen	Air or oxygen	Air, nitrogen, or oxygen	Air, nitrogen, or oxygen	Air	Oxygen
Outer gas flow, ℓ/min	25.0	19—22	20.0	20.0—24.0	14.0	15.0
Intermediate gas flow, ℓ/min	3.5	2.6—2.8	1.2	1.0—3.0	0.8—1.0	0.5
Injector gas flow, ℓ/min	1.5	0.5—0.7	1.0	0.8—1.0	0.7—1.2	0.7
Plasma configuration	Annular	Annular	Annular	Annular	Annular	Annular

[a] c.c., crystal controlled generator.
[b] G, Greenfield torch; F, Fassel torch; MAK, low-gas torch (manufactured by Sheritt Gordon Mines, Ltd. of Canada).
[c] u.s., unspecified.

Table 4
EQUIPMENT AND OPERATING CONDITIONS USED FOR ICPs OPERATED IN PURE HELIUM

References	73	74	75	75	76, 77
Equipment					
Generator model	R.C. Durr	R.C. Durr	Plasma-Therm 5000 D	Plasma-Therm 5000 D	Plasma-Therm 5000 D
Generator type[a]	t.l.o.	t.l.o.	c.c.	c.c.	c.c.
Frequency, MHz	50.0	54.0	27.0	27.0	27.0
Torch type[b]	Demountable (12 mm I.D.)	Demountable (12 mm I.D.)	F or low-gas flow	Modified F	Low-gas flow
Nominal power, kW	6.0	6.0	5.0	5.0	5.0
Operating conditions					
Forward power, kW	0.6	0.6	0.7	1.0	1.5
Observation height, mm	u.s.[c]	u.s.	n.a.[d]	5.0	25.0
Outer gas flow	15 air (external)	15 air (external)	0	55.0	7.0
Intermediate gas flow, *l*/min	0.2	1.2	8.5	0	n.a.
Injector gas flow, *l*/min	0.2	0.8	2.0	1.8	1.0
Plasma configuration	Filament	Filament	Hollow	Annular	Annular

[a] t.l.o., tuned-line oscillator with 50-kV overpotential; c.c., crystal control generator.
[b] F, Fassel torch.
[c] u.s., unspecified, within load coil.
[d] n.a., not applicable.

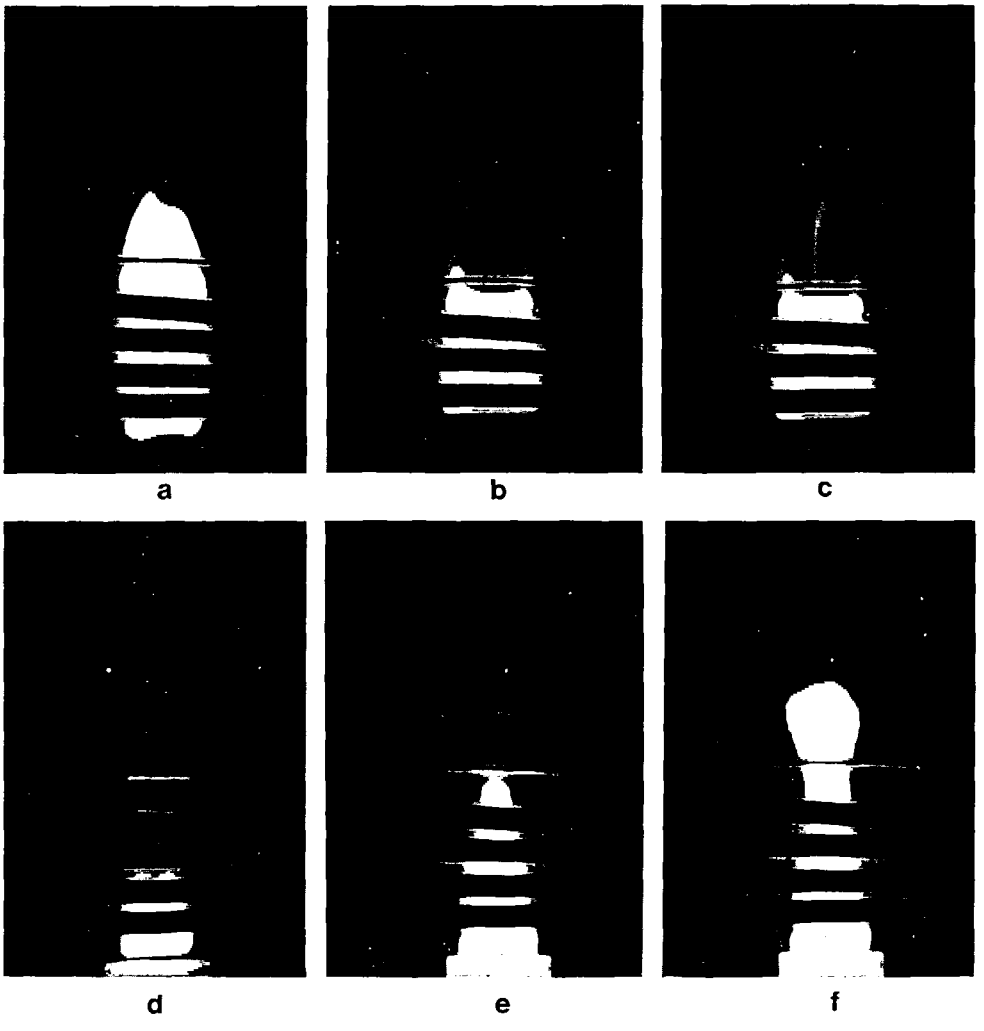

FIGURE 1. Ar ICP (a); Ar-N_2 ICP using pure N_2 injector gas flow (b) and (c); 1000 μg/mℓ of Y solution was nebulized into the plasma in c; Ar-N_2 ICP with pure N_2 outer flow as a function of forward power (d—f); d, 2000 W; e, 3000 W; f, 4000 W. (From Montaser, A., Fassel, V. A., and Zalewski, J., *Appl. Spectrosc.*, 35, 292, 1981. With permission.)

replace Ar in the outer flow.[6,17,38,57-59,61,62,64] Again, such changes are best defined on a quantitative basis by the plasma temperature, but this fundamental parameter has not often been measured to explain the observed trends. The reduction in axial channel diameter enhances sample-plasma interaction, thereby reducing possible solute vaporization interference effects.[60,64] The reductions in apparent volume have been interpreted in terms of the energy needed to dissociate diatomic molecule.[6,38] As a result of the dissociation, reduced temperature and diminished electron number densities[16,18] are expected in the outer region of the discharge. This thermal pinch effect has also been explained in terms of gas transport properties such as thermal conductivity and specific heat.[33,40,80,83-85] In contrast to Ar, the thermal conductivity of nitrogen does not increase monotonically with temperature, but rather, it reaches a maximum at 6500 K, falls to a minimum at about 9000 K, and again begins to rise with increasing temperature. Thus, the radial temperature of an Ar-N_2 ICP discharge may pass through an

inflection point similar to the effect predicted for a nitrogen plasma,[84] and the discharge appears smaller.

Among molecular gases used in the outer flow of the ICP discharge, nitrogen has been the one most commonly used.[6,16,18,20,23,25,29,31,38-43,46-53,56-66,86-94] The procedures for introducing nitrogen into the Greenfield and Fassel torches are slightly different. An intermediate gas flow of Ar is required when nitrogen or other molecular gases are introduced in the outer flow. The Greenfield torch (25 mm I.D.) is usually ignited[6] when only the intermediate gas passes through the torch at a rate of 10 to 35 *l*/min of Ar. After plasma formation, nitrogen is immediately introduced in the outer flow at a rate of 20 to 70 *l*/min[6] and the sample may then be injected by means of the injector gas. For the Fassel torch (18 mm I.D.), the normal torch position is raised by about 2 mm with reference to the load coil and an Ar ICP discharge is generated by the commonly used procedure.[95] After adjusting the intermediate gas flow rate to 2.5 *l*/min, the outer Ar flow is gradually replaced with the nitrogen flow until a pure nitrogen outer flow is established.[57,58,62]

For the torches described above, the apparent plasma volume increases linearly with forward power.[40,57,61] Typical changes in shape that result from increases in forward power and the nitrogen outer flow rates are shown photographically in Figure 1d, e, and f for ICP discharges generated in the Fassel torch.[57] In general, the power required to operate a plasma depends on the gas type, the gas flow rate, and the type of torch used. For example, when pure nitrogen is used as the outer gas flow of an Ar-N_2 ICP discharge, the Greenfield torch (25 mm I.D.) should be operated at forward powers greater than 2.5 kW and at outer, intermediate, and injector gas flow rates of 20 to 70 *l*/min of N_2, 10 to 35 *l*/min of Ar, and 2 to 3 *l*/min of Ar, respectively.[6] If a Fassel torch is used to generate the same plasma,[16,18,57,58,60,62-64] power and gas requirements are generally reduced, as shown in Table 2, compared to those for a Greenfield torch. Ebdon et al.[50] optimized dimensions of the Greenfield torch to reduce its gas and power requirements for forming both Ar and Ar-N_2 ICP discharges. Thus, torch design is quite critical in operating relatively low-power mixed-gas and molecular-gas ICPs. Further reduction in both power and gas requirements may be achieved when a low-gas-flow torch is used.[65,66,89]

An oxygen outer flow has been used to generate Ar-O_2 ICP discharge in the Greenfield[55] and Fassel-type torches.[18,61,63,64] Power and gas-flow requirements were similar, Table 2, to those of an argon-nitrogen ICP, but a larger apparent volume was observed for Ar-O_2 ICP discharge as compared to the Ar-N_2 plasma.[55,61,62] As a result of oxygen dissociation, the Ar-O_2 ICP discharge emitted a blue radiation.

Argon-air ICP discharges, with air outer flow, have also been formed in the Greenfield torch with generators operated at frequencies of 9[44,45] and 27 MHz[56] and in a Fassel torch at 27 MHz,[18,61,63,64] Table 2. In general, the Ar-air plasma was shorter than an Ar ICP discharge when the plasmas are generated in the Greenfield[44] or Fassel[61,62] torches, but a brighter, longer, conical plasma was obtained[56] for the Ar-air ICP discharge compared to the Ar-N_2 ICP discharge using a pure nitrogen outer flow. No reports on Ar-air and Ar-O_2 ICP discharges, generated in low-gas-flow torches, have appeared yet. Work in this area is currently in progress in our laboratory.

Reports on the use of hydrogen in analytical ICP discharges have been very limited. A mixture of 93.5% Ar and 6.5% H_2 has been used[34,35,81] for the outer gas flow of the Fassel torch. The improvement in the observed detecting power of the Ar-H_2 ICP discharge has been partially attributed to the unspecified geometric variation of the discharge brought about by hydrogen.[34] Presumably, a thermal pinch has been observed for the Ar-H_2 ICP discharge, similar to that reported for an Ar-H_2 plasma used for induction heating.[80] This thermal pinch effect has also been observed when the

outer flow of an Ar ICP discharge contained only 0.3% H_2.[17] As discussed in Section V.A.2, Batal et al. reported higher electron number density and excitation temperatures for the Ar-H_2 ICP discharge compared to the Ar ICP discharge.[17]

An Ar-He ICP discharge with 70% He and 30% Ar in the outer flow was operated in the Fassel torch.[18,61-64] The Ar-He plasma was slightly smaller but significantly less intense than the Ar discharge. Introduction of greater than 70% He into the outer flow extinguished the plasma.[18,61-64] Meyer and Barnes[69] were able to introduce up to 95% helium into their plasma generated in a special torch. Relatedly, Chan and Montaser[75] introduced 100% He in the outer flow of an Ar-He ICP, but the plasma configuration changed from an annular to a long, filament-type discharge.

D. ICP Discharges with Pure Molecular Gases

For the plasmas reviewed so far, Ar has been used in at least one of the three gas flows of the ICP torch. The ICP discharges to be discussed below (Table 3), are sustained in only pure molecular gases such as nitrogen, oxygen, or air. No reports on molecular-gas ICP discharges, generated in the Greenfield torch, have been published so far.

The procedure for the generation of molecular-gas ICP discharges in a Fassel-type torch and a demountable torch,[69] having a boron nitride injector tube, was described by Meyer et al.[26,67-71] For example, to initiate the N_2 discharge, an Ar ICP discharge was first formed and the impedance matching network was adjusted to a predetermined value suitable for a N_2 discharge.[26] Nitrogen was then introduced in the outer flow until the discharge volume remained unchanged. This step was followed by introducing nitrogen injector gas while simultaneously reducing the argon outer flow. Finally, the intermediate nitrogen flow was introduced to prevent damage to the intermediate quartz tube. The annular N_2 ICP discharge was reported to form in less than a minute.[26,67-71] The N_2 ICP discharge[67] had a triangular shape and was less intense than the Ar-N_2 ICP discharge. Recently, Meyer used a commercial low-gas-flow torch[96] to generate an air ICP discharge,[27] and Barnes and Yang[72] reported formation and characteristics of an O_2 ICP discharge generated in a conventional torch. The conversion from pure Ar to air or O_2 ICP discharge was simplified to a one-step process by using 41-MHz generators.[27,72] An air-ICP atomic emission spectrometer, designed for process-controlled applications, has been introduced into the marketplace by the Baird Corporation.

Compared to an Ar ICP discharge, nitrogen and air plasmas extend further beyond the load coil, but they are less intense.[26] In general, postdischarge temperatures of molecular-gas plasmas are higher, owing to a relatively minor cooling by ambient air, than those of an Ar ICP discharge. This extended tail flame for a molecular-gas ICP discharge. should increase plasma-sample interactions and should be advantageous for direct analysis of solid samples.

E. Helium ICP Discharges

Because of the high electrical resistivity and high thermal conductivity of He vs. Ar, the generation of He ICP discharges has been more difficult than for Ar plasmas. To simplify the plasma formation, the He ICP discharges have been formed at reduced pressure,[97-100] but the applications of these plasmas are limited to gas analysis. At atmospheric pressure, He ICP discharges have been generated by Mermet and associates[73,74] and Montaser and co-workers.[75-77] The operating conditions for various helium ICP discharges are listed in Table 4. Abdallah and Mermet[73] utilized a special generator that could provide 50 kV overpotential to the load coil and that possessed a

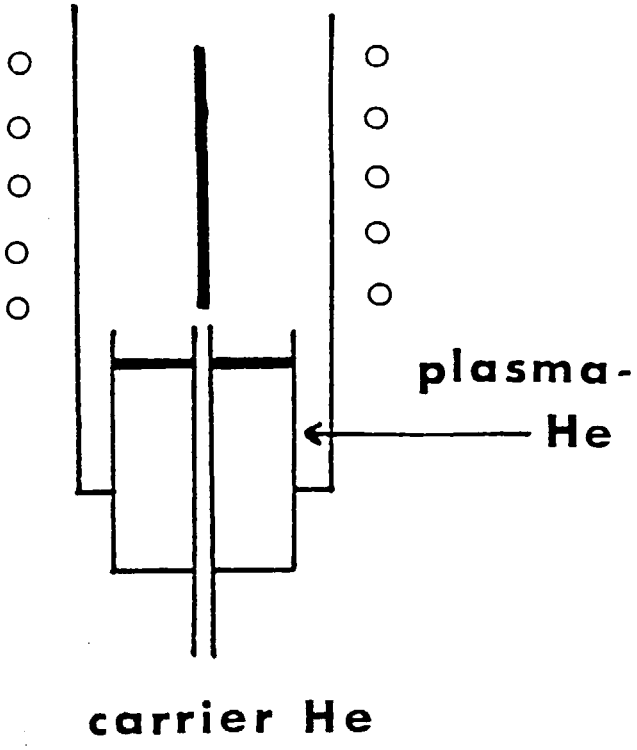

FIGURE 2. Demountable torch used for generating a filament-type He ICP. (From Robin, J., *Prog. Anal. At. Spectrosc.*, 5, 79, 1982. With permission.

very high Q factor. The helium plasma[73,74] was stabilized in a specially fabricated torch that was cooled externally by air (Figure 2). As shown in Figure 2, the He ICP discharge was confined to the induction region and resembled a 3-mm-wide filament surrounded by a high temperature glow. No axial channel for this plasma was observed.

Two types of He ICP discharges were formed by Chan and Montaser[75] using a commercially available Ar ICP facility. The hollow He ICP discharge, Figure 3A and B could be initiated in a flowing stream of pure helium in a Fassel torch with extended outer tube[101] or a low-gas-flow torch.[96] The blue discharge of the He ICP extended 1.5 cm above the load coil, and it touched the side of the outer tube. The annular He ICP discharge (Figure 3D, E, and F), was generated when helium was gradually introduced into the outer flow of an Ar ICP. A Fassel torch with an extended outer tube was used to generate the plasma. As the helium flow rate was increased to 55 *l*/min, the teardrop-shaped Ar ICP changed into a filament-type, argon-helium discharge. After the Ar outer flow was turned off, a pure filament-type helium ICP was formed, Figure 3C. The bluish-white filament, surrounded by a blue glow, was 5 mm in diameter and was extended to a height of about 5 cm above the load coil. When helium injector gas was introduced and the forward power was increased to 1.0 kW simultaneously, the plasma radiation became pinkish-red and an annular helium ICP discharge was formed. For the annular He ICP, the width of the plasma was about 8 mm and sample aerosol could be injected into the discharge without any difficulty.[75] Montaser and associates[76,77] have recently reduced the total He gas flow to 8 *l*/min for an annular He ICP generated in a unique low-gas-flow torch.

III. SPECTRAL FEATURES

To evaluate the analytical performance of the various ICP discharges, a compilation

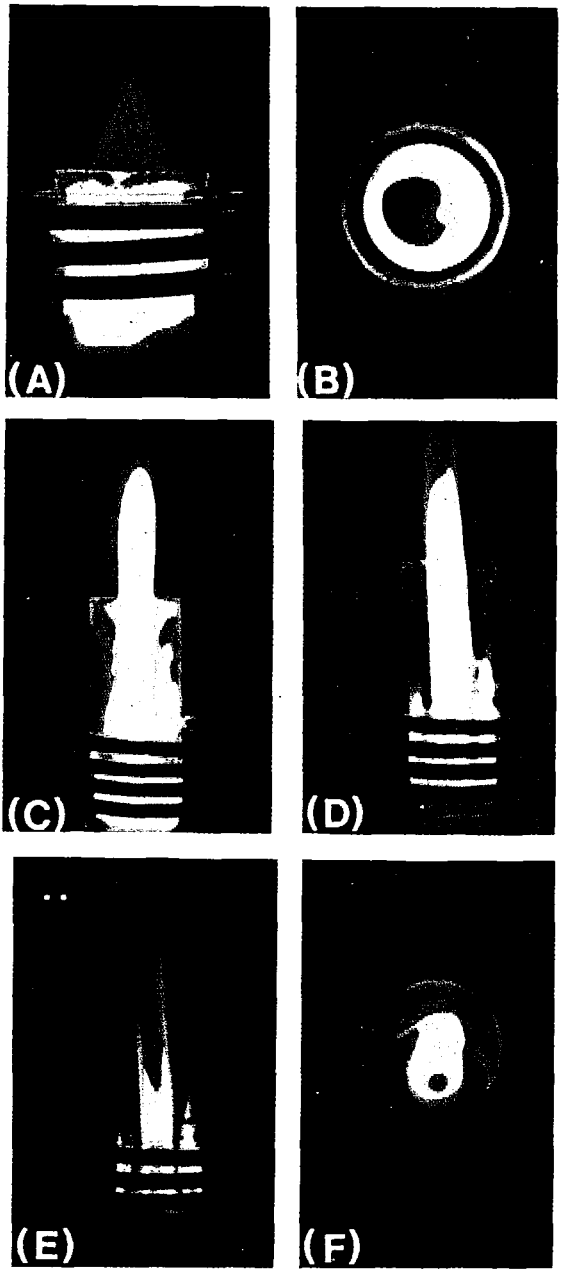

FIGURE 3. Hollow He ICP generated in a low-gas-flow torch (A) and (B), side and top views, respectively; filament-type He ICP (C); annular He ICP, side view taken at different exposure (D) and (E); annular He ICP (F), top view taken at an angle. Plasmas in Figures C to F are generated in a modified Fassel-type torch using an extended outer tube. (From Chan, S. and Montaser, A., *Spectrochim. Acta*, 40B, 1467, 1985. With permission.)

has been made of the spectral wavelengths of the atomic lines and molecular bands emitted by different gases in the plasmas. In general, mixed- and molecular-gas ICP discharges possess more complicated spectra than Ar plasmas. A list of important molecular band systems observed in mixed-gas and molecular-gas ICP discharges is given in Table 5 and in Figures 4 and 5.[68,70]

The most intense band spectrum of the nitrogen ICP discharge is the first negative system (FNS) of N_2^+ molecules and the second positive system (SPS) of N_2 molecules, while for the air ICP discharge, the NO band exhibits the greatest intensity. For the O_2 ICP, the Schumann-Runge system of O_2, especially the {0,14} bandhead, is the most intense one.[68] The bandhead of the first positive system (FPS) of N_2 lies at 1049 nm, which is too far in the infrared region to be observed by typical ICP spectrometers, yet other bands of this system have been recorded below 650 nm.[33] Certain bands such as C_2, CN, and CO may only be eliminated in the Ar-O_2[91] or oxygen ICP discharges.

The spectra of argon, nitrogen, and air plasmas (Figure 4), clearly document the relative complexities of the radiation emitted by the ICP discharges in the 180- to 550-nm region.[70] Compared to Ar and air plasmas, where NO band emission is observed in the wavelength region of 180 to 280 nm, no spectral transition occurs in the same region in the high-power, nitrogen ICP discharge.[70] Relatedly, while only weak emission is recorded for nitrogen and air plasmas in the region of 430 to 580 nm, strong Ar atomic lines are emitted from Ar ICPs. Also, the continuum intensities measured for nitrogen and air ICP discharges at 3.5 kW are lower, especially at high wavelengths, than the background continuum for a 1.0 kW Ar ICP.[26,70] For example, the background continuum measured at about 560 nm for nitrogen and air ICPs can be 10 to a 100 times lower, respectively, than the values obtained for the commonly used Ar ICP discharge.[26,70] Thus, S/B ratios and detection limits measured in molecular gas plasmas at high wavelength are anticipated to be superior to those achieved for the Ar ICP discharge.

The use of 41-MHz instead of 27-MHz generators enables the operation of molecular-gas ICP discharges at 1.5 to 2.0 kW rather than at 3- to 3.5-kW power levels, thereby reducing the continuum background levels emitted by the plasmas. However, the complexities of the spectra emitted by the plasmas are hardly altered as a result of the use of lower power at higher frequencies (Figure 5). A comparison of the spectra for nitrogen, air, and oxygen in Figures 4 and 5 indicates that as far as spectral interferences are concerned, the air ICP discharge is the plasma of choice for analyte spectral lines emitted at wavelengths greater than 280 nm, while the nitrogen plasma is superior at wavelengths less than 280 nm. In general, the choice of molecular-gas discharge is entirely dependent on the spectral lines of interest.

In terms of spectral features, the molecular bands observed in mixed-gas ICPs[57,63] are quite similar to those recorded for molecular-gas discharges. The emission spectra of Ar-O_2 and Ar-N_2 ICP discharges using pure molecular gases in the outer flow[55] are shown in Figure 6. Similar to the N_2 ICP discharge, the continuum background is relatively flat at wavelengths less than 280 nm, but above 350 nm, the Ar-O_2 plasma exhibits a less structured background. The superiority of Ar-O_2 plasma over Ar-N_2 ICP discharge in the simplification of spectra of transition elements is demonstrated in Figure 7 for the determinations of Zr and La.[55] In contrast to Ar-N_2 ICP, relatively flat backgrounds are obtained around Zr 343.8 and La 379.4 lines if Ar-O_2 is used, thus enhancing the selectivity of the measurement. The Ar-air ICP discharge[56,61,63] exhibits the combined spectral features of Ar-N_2 and Ar-O_2 plasmas.

An Ar-He ICP discharge[61,63] was reported to exhibit a lower background continuum compared with an Ar ICP. Because of the reduced intensity of the Ar-He ICP com-

Table 5
TRANSITIONS OF SPECIES OBSERVED IN MIXED-GAS AND MOLECULAR-GAS ICPs

Band system	Transition[a]	(0,0) Bandhead, nm[a] (band range, nm) [observed range, nm]	Ref.
1. First negative system (FNS) of N_2^+	$B^2\Sigma_u^+ - X\ ^2\Sigma_g^+$	391 (329—586) [330—470]	26, 30, 33, 38, 39, 44, 51, 56, 58, 61, 63, 66—68, 91
2. Second positive system (SPS) of N_2	$C^3\Pi_u - B^3\Pi_g$	337 (281—497) [315—426]	26, 30, 33, 38, 51, 56, 58, 66—68, 91
3. First positive system (FPS) of N_2	$B^3\Pi_g - A^3\Sigma_u^+$	1051 (503—1051) [<650]	26, 33
4. NO gamma	$A^2\Sigma^+ - X^2\Pi$	226 (195—345) [203—284]	26, 30, 58, 61, 63, 68
5. Schumann-Runge system of O_2	$B^3\Sigma_u^- - X^3\Sigma_g^-$	Unknown (176—437) [220—380]	30, 38, 63, 68
6. Second negative system of O_2^+	$A^2\Pi_u - X^2\Pi_g$	262 (205—610) [280—450]	38, 91
7. CN Violet	$B^2\Sigma^+ - X^2\Sigma^+$	388 (358—460) [358—450]	26, 31, 32, 38, 59, 61, 63, 66, 68, 86, 91
8. NH	$A^3\Pi - X^3\Sigma^-$	366 (302—380) [336—337]	30, 38, 68, 91
9. OH	$A^2\Sigma^+ - X^2\Pi$	306 (306—325) [280—325]	30, 38, 91
10. C_2 Swan	$A^3\Pi_g - X^3\Pi_u$	516 (436—667) [467—619]	31,32,86,91
11. CO Asundi	$a^3\Sigma - a^3\Pi$	Unknown (547—859) [711—721]	91
12. CO^+ Baldet-Johnson	$B^2\Sigma^+ - A^2\Pi$		38[b]
Comet tail	$A^2\Pi - X^2\Sigma^+$	397 (308—640) [337—420]	38[b]

[a] From References 102 and 103.
[b] The two-band systems are not distinguished from each other.

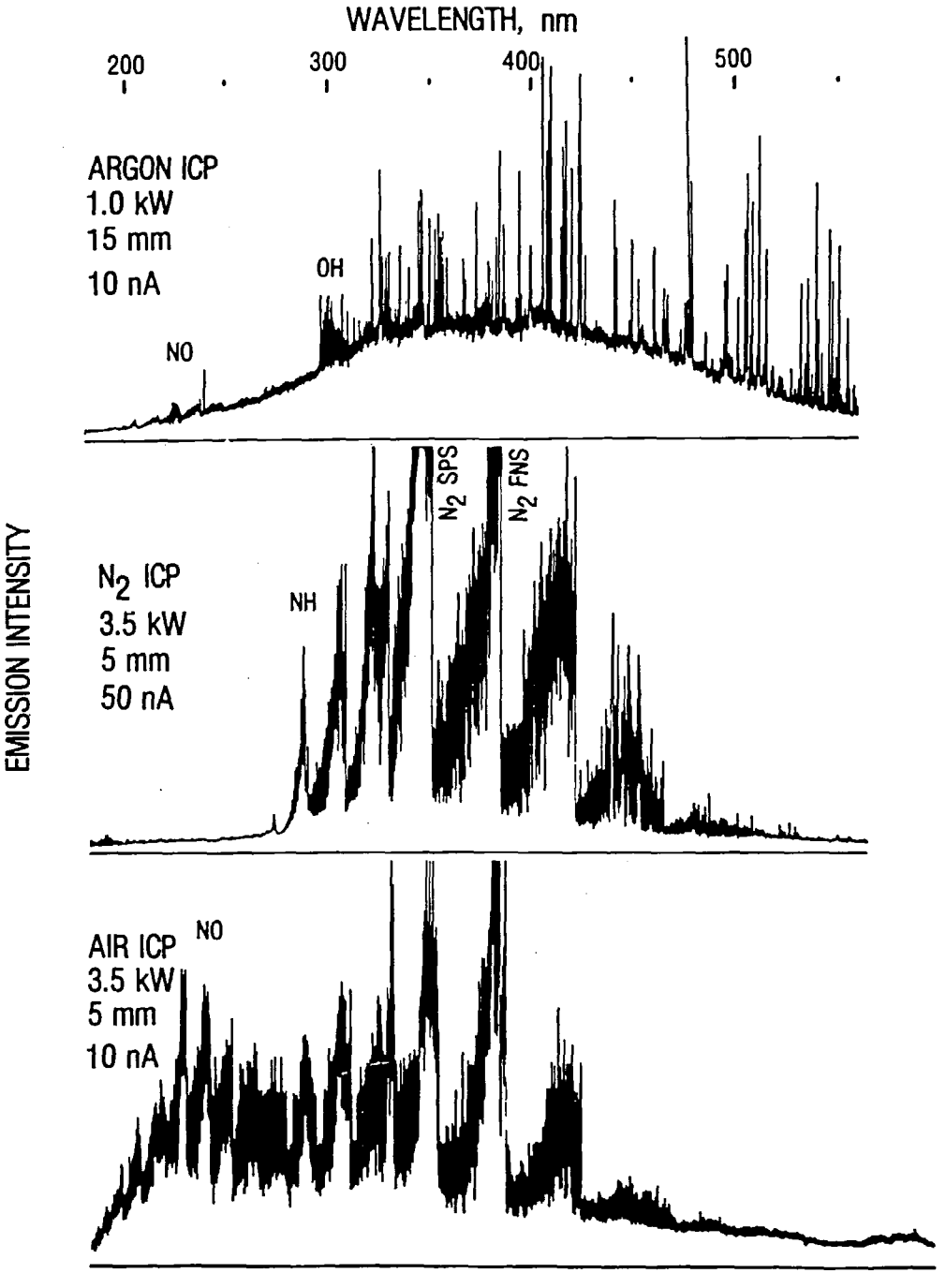

FIGURE 4. Background emission spectra of analytical argon, nitrogen, and air ICPs. (From Meyer, G. A., Ph.D. dissertation, Department of Chemistry, University of Massachusetts, Amherst, 1982. With permission.)

pared to an Ar plasma and the absence of emission from He atom, He ion, and molecular bands such as N_2^+, Choot and Horlick[61,63] concluded that the Ar-He ICP discharge lacked the energy to excite many species. To our knowledge, background spectra for hydrogen gas introduced into the plasma have not yet been reported for ICP discharges used in analytical laboratories.

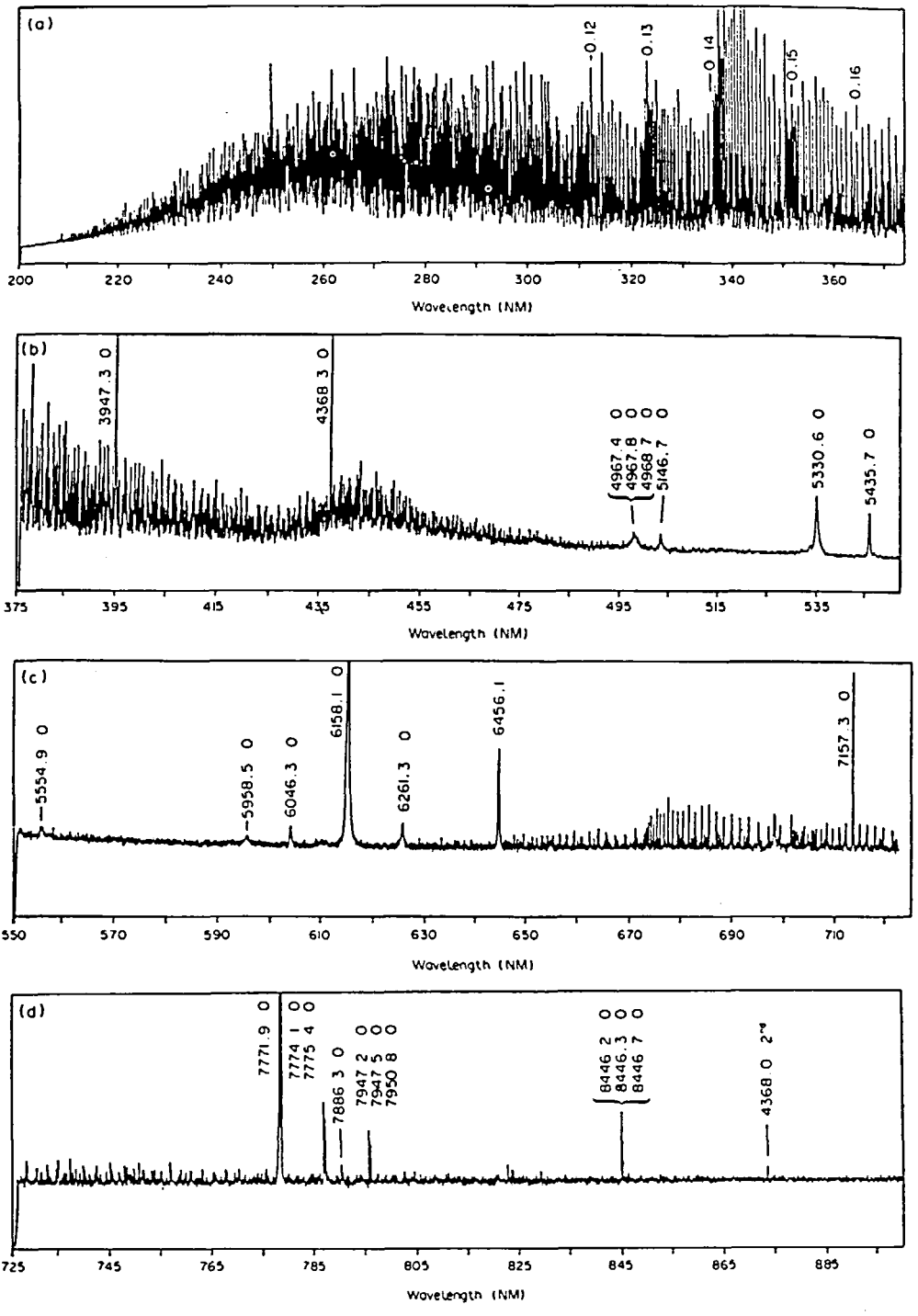

A

FIGURE 5. Background emission spectra of 2-kW (A) oxygen and (B) air ICPs recorded at observation heights of +2 and +5 mm, respectively, above the load coil: recorded between 200 and 375 nm (a); recorded between 375 and 550 nm (b); recorded between 550 and 725 nm (c); and recorded between 725 and 900 nm (d). (From Meyer, G. A. and Thompson, M. D., *Spectrochim Acta*, 40B, 195, 1985. With permission.)

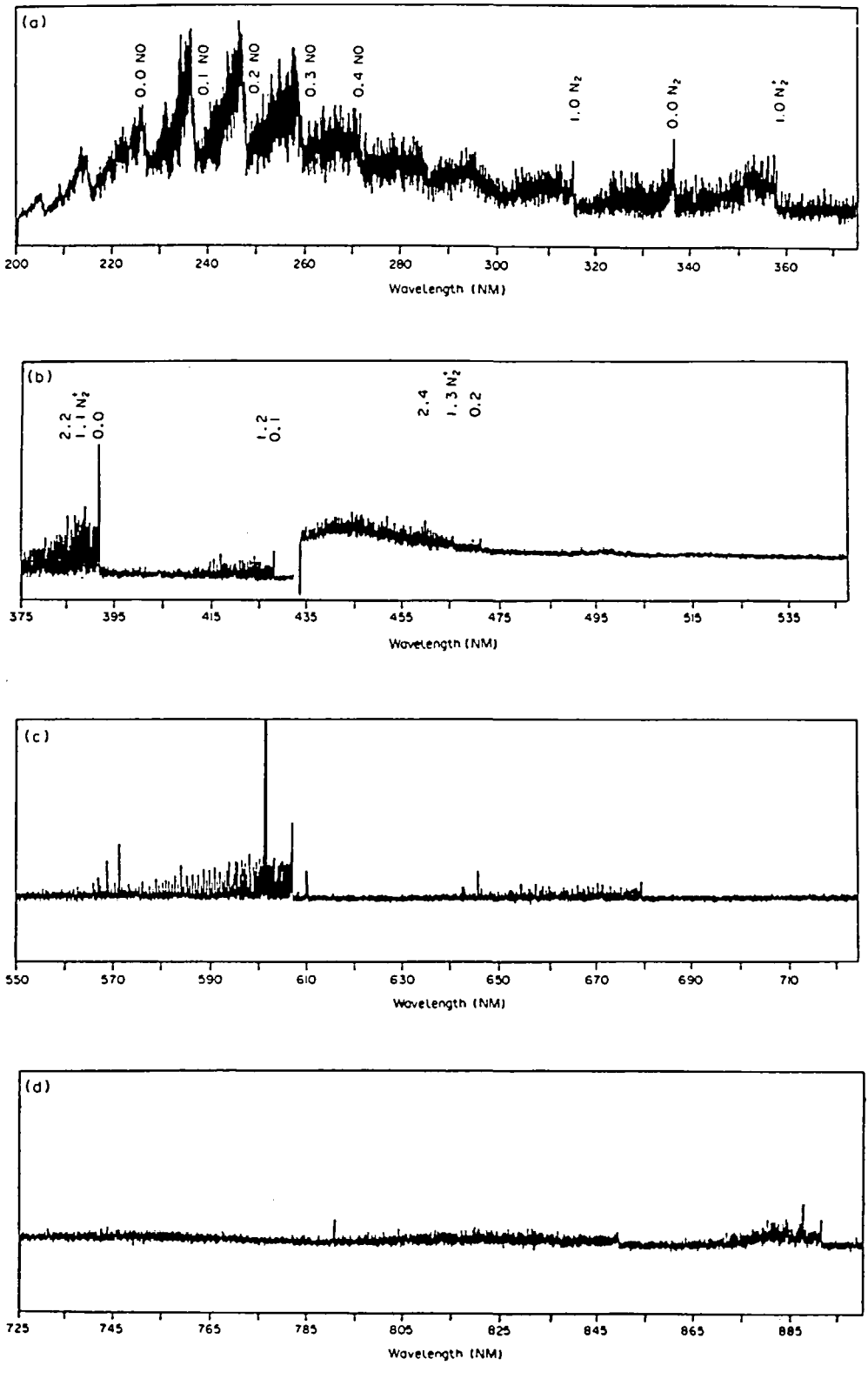

FIGURE 5B.

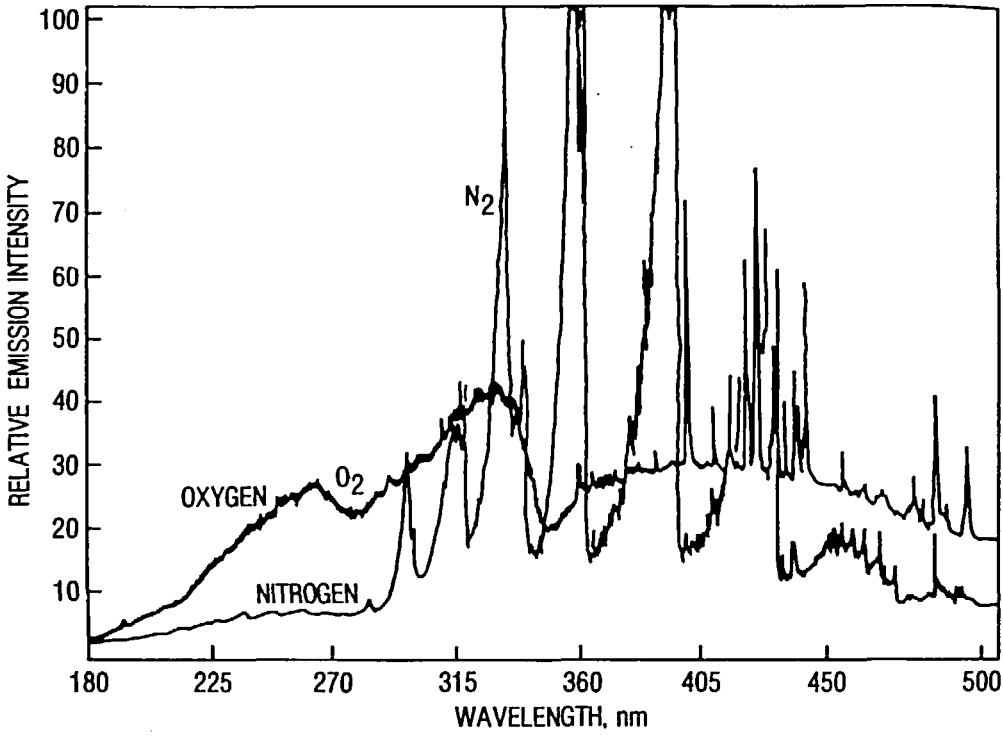

FIGURE 6. Background emission spectra of Ar-O_2 and Ar-N_2 ICPs: forward power, 2.8 kW; outer flow rate, 16 *l*/min of N_2 or O_2; intermediate flow rate, 9 *l*/min of Ar; injector gas flow rate, 0.3 to 0.4 *l*/min of Ar; observation height, 8 mm. (From Ohls, K. and Sommer, D., *ICP Inform. Newsl.*, 9, 555, 1984. With permission.)

IV. ANALYTICAL PERFORMANCE OF PLASMAS

A. Optimization Strategies

A meaningful interlaboratory comparison of analytical performance of plasmas generated with different gases is possible only if the ICP discharges are operated under optimized conditions. To compare the plasmas, net intensities,[57,59,63,64] S/N,[57,62-64] and S/B[57,60,104] ratios are typically used as the appropriate figures of merit. The goal of the optimization, especially for simultaneous multielement determinations, may also focus on the achievement of minimum ionization interference[104] or the attainment of minimum spectral interference or maximum selectivity.[105]

In our opinion, the use of net analyte intensity as the sole figure of merit for characterizing plasmas[59,63,64] is not advisable because background variations are neglected. Montaser et al.[57] have clearly demonstrated that introduction of 5 to 20% N_2 in the outer flow of an Ar-N_2 ICP discharge enhances *both* the net analyte and background intensities. In such cases, the real gain in the analytical performance of mixed-gas plasmas may be marginal. Relatedly, the use of S/N ratios, based on measurements of precision of analyte intensities,[63,64] may also mislead the analyst in comparing the detection capabilities of the plasmas, because differences of plasma backgrounds are not considered. A more realistic estimate of S/N ratios may be obtained by measuring the precision of the background,[57] yet such measurements are subject to scatter. Because

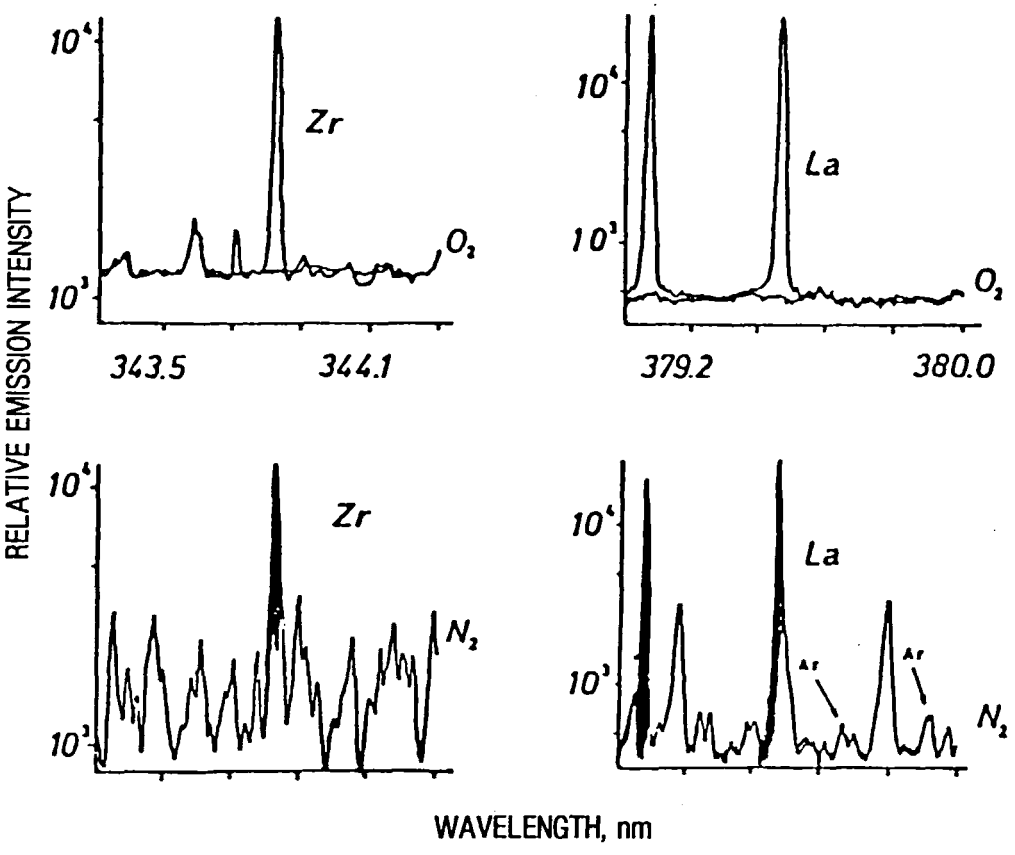

FIGURE 7. Emission spectra of Zr and La in Ar-O_2 and Ar-N_2 ICPs. Same operating conditions as Figure 6. (From Ohls, K. and Sommer, D., *ICP Inform. Newsl.*, 9, 555, 1984. With permission.)

of its larger statistical variation, the S/N ratio is less often used compared to the S/B criteria for optimization studies.[57,60,104]

The S/B and S/N values of elements in an ICP discharge are functions of several parameters, such as observation height, forward power, various gas flows for the ICP torch, and the spectral line selected. To obtain the true optimum operating condition, all of these parameters must be altered relative to one another. During the early stages of the development of ICP-based methods, the sequential optimization technique, in which one variable is changed at a time while the others are held constant, was often used. The primary disadvantages of the sequential approach are the necessity of conducting a large number of experiments and the unreliability of the derived optima.[41,57] To minimize these problems, the modified simplex optimization technique has recently been increasingly used,[26,35,45,50,60,104] particularly in the applications of Ar-N_2 ICP discharges. The simplex approach allows simultaneous variation of all parameters, thereby requiring substantially fewer experiments to reach the optimum conditions. Details of the simplex optimization technique[106] and its application in simultaneous multielement analysis[107] are given elsewhere. Parker et al.[108] compared speed and accuracy of various simplex algorithms for optimizing experimental conditions of ICP emission spectrometric studies.

B. Effect of Operating Conditions on Analytical Results

The use of simplex optimization eliminates the need for obtaining detailed informa-

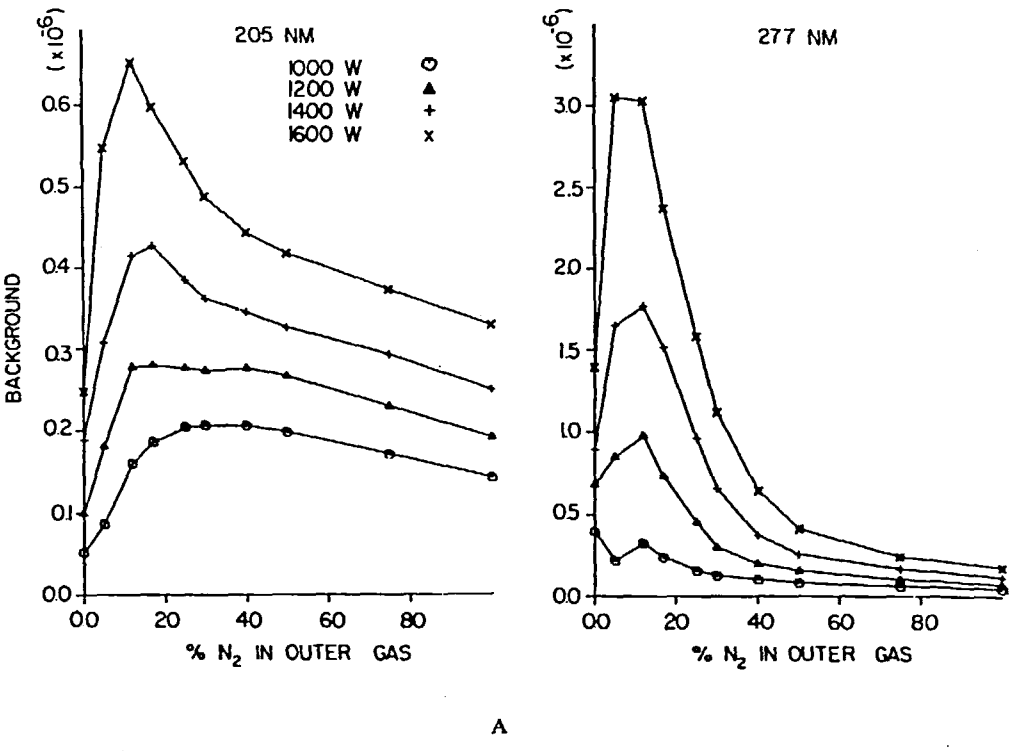

FIGURE 8. The effect of operating conditions for an Ar-N_2 plasma generated in the Fassel-type torch. Forward power and percent nitrogen in the outer flow on background (A) and net analyte (B) intensities; observation height and percent nitrogen in the outer flow on the relative intensities of Ni atom and ion spectral lines (C). (From Montaser, A., Fassel, V. A., and Zalewski, J., *Appl. Spectrosc.*, 35, 292, 1981. With permission.)

tion on the variation of analyte signal with different parameters. However, to understand fundamental processes in plasmas, it is instructive, especially for mixed-gas ICP discharges, to examine the effects of individual parameters on the signal.

In terms of analytical performance, the Ar-N_2 ICP has been investigated more extensively than other mixed-gas and molecular-gas ICP discharges. The typical influence of forward power, observation height, and percent nitrogen in the outer flow of an Ar-N_2 ICP on background emission, analyte emission, and S/B ratios is shown in Figures 8 and 9. Two important conclusions can be drawn from these figures. First, the highest background, net analyte intensity, and S/B ratios are achieved when the outer gas contains 5 to 25% nitrogen.[57] Second, while the background, the net intensity, and the S/B values decrease sharply for ion lines as the outer gas flow approaches 100% nitrogen, the opposite trend is found for the neutral atom lines of medium excitation energies.[57] The disparity between the behavior of atom and ion lines suggests that different excitation mechanisms prevail for these species in mixed-gas ICP discharges.

The above conclusions achieved from the studies of Montaser et al.[57] have been reconfirmed by Choot and Horlick,[62-64] who also introduced O_2, air, and helium into the outer flow of the Fassel torch. Their best results, shown in Figure 10, clearly indicate that mixed-gas plasmas exhibit maximum intensities at an observation height of 10 mm, where the analyte intensity in the mixed-gas plasma is a factor of 2 to 3 greater than that of an Ar ICP discharge. These observations, also noted when hydrogen[17,34,35] was added to the outer flow, may be correlated with the increase in electron number densities measured in mixed-gas ICPs.[17,18,61] More importantly, Choot and Horlick[63]

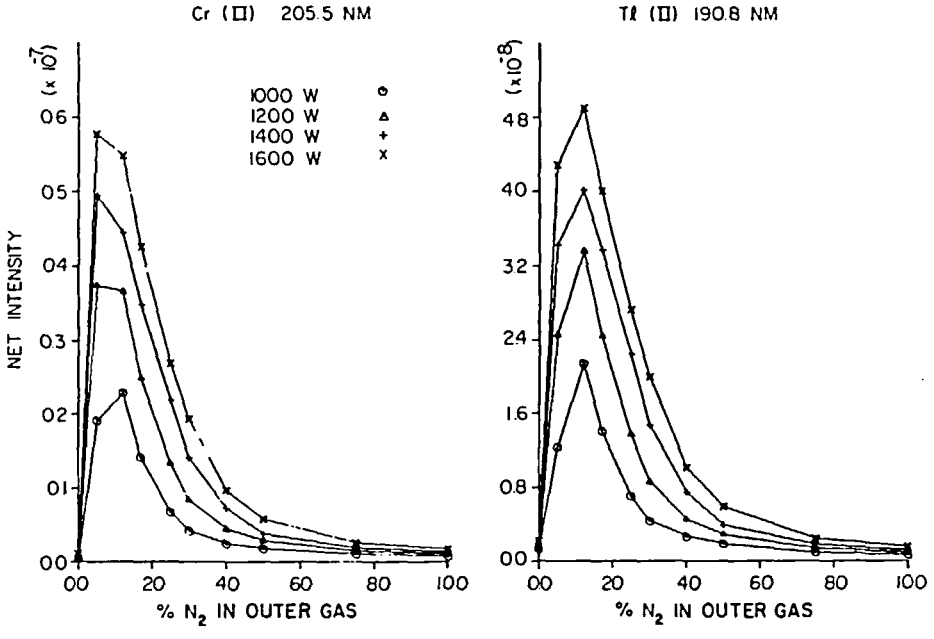

FIGURE 8B.

also found that when air, pure nitrogen, pure oxygen, or a mixture of 70% He and 30% Ar was used in the outer flow of the plasma, the S/N ratios measured for three high-excitation-energy cadmium lines, even at a forward power of up to 2.3 kW, were inferior, by a factor of 3 to 4, to those achieved for an Ar ICP discharge. However, when the Ca II 393.4-nm line was observed, the S/N ratios measured for the Ar plasma and for the mixed-gas ICP discharge, using pure molecular gases in the outer flow, were equivalent. Definite conclusions on the comparative analytical performance of the plasmas cannot be achieved unless further studies are conducted to evaluate mixed-gas plasmas at higher forward power levels. Obviously, such studies must be performed with many test elements covering a wide wavelength range. As far as we know, this study has only been conducted for Ar-N_2 ICP discharges.[57,60,104]

Introduction of molecular gases into the injector gas of the Ar ICP discharge generally reduces the continuum background in the axial channel[32,57] and analyte emission intensities,[29,30,32,57] although the plasma requires higher power, compared to pure Ar ICP, for stable operation. Thus, Greenfield and associates[29] found that analyte emission intensity decreased in the order Ar > N_2 > air > O_2 for the injector gas. In the study of the behavior of 20 atom and ion lines, Montaser et al. reported the rapid reduction of background, net intensities, S/B, and S/N values as nitrogen replaced argon in the injector gas (1 *l*/min) of an Ar-supported ICP.[57] The greatest deterioration in S/B values, and thus, the detection limits, was observed[57] for spectral lines of high excitation energies (hard lines) rather than for neutral atom lines, such as Cr 357.8 nm, Co 345.3 nm, Mo 386.4 nm, Ni 341.4 nm, and Tl 377.5 nm, which possess medium excitation energies (soft lines). A similar trend was observed for the Ca II 393.3-nm line when the argon injector gas flow of an Ar-N_2 ICP discharge, with a pure N_2 outer flow, was partially replaced with N_2.[61,62] In contrast, Meyer and Barnes[26] reported that the use of an air injector gas in an Ar-air ICP, at simplex optimized conditions, provided S/B and detection limits which were nearly comparable to the results for an Ar ICP for both calcium atom and calcium ion lines. For these results, lower forward

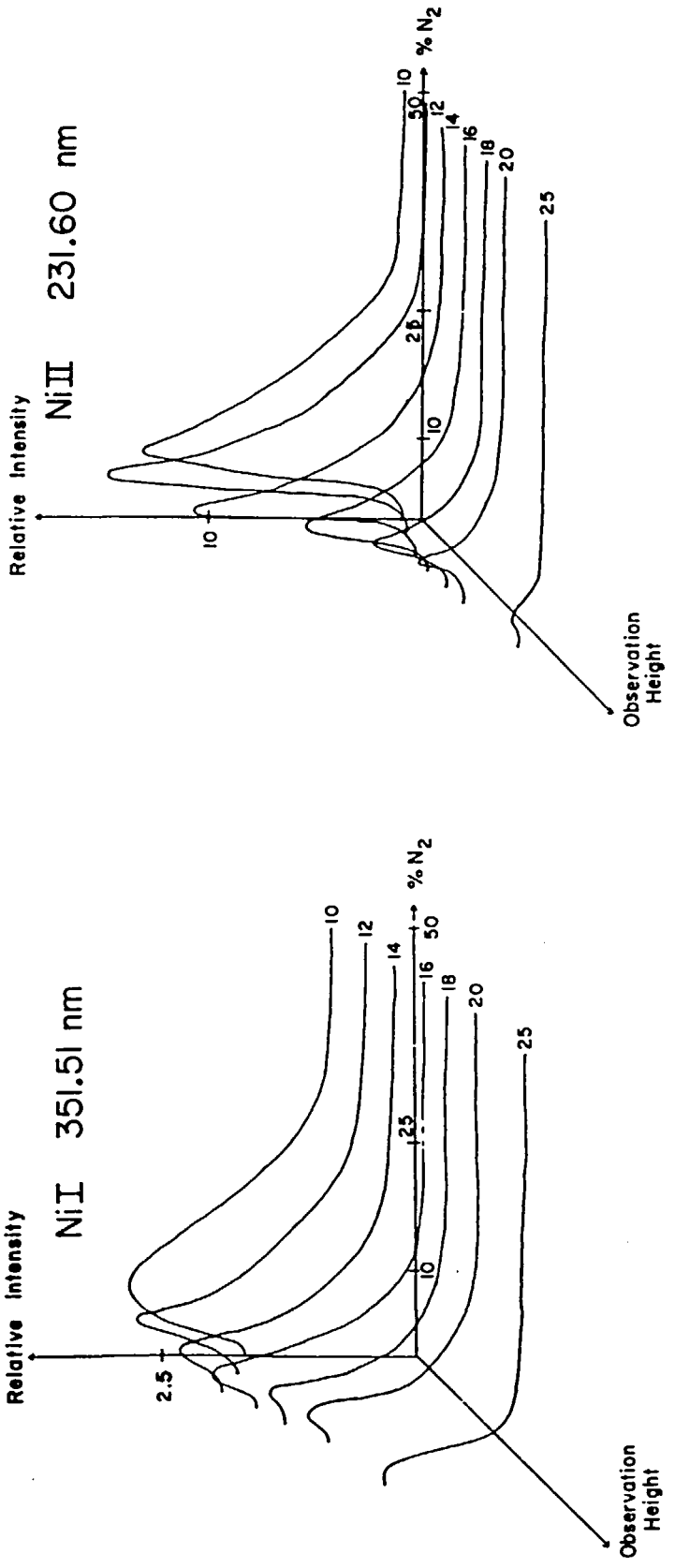

FIGURE 8C.

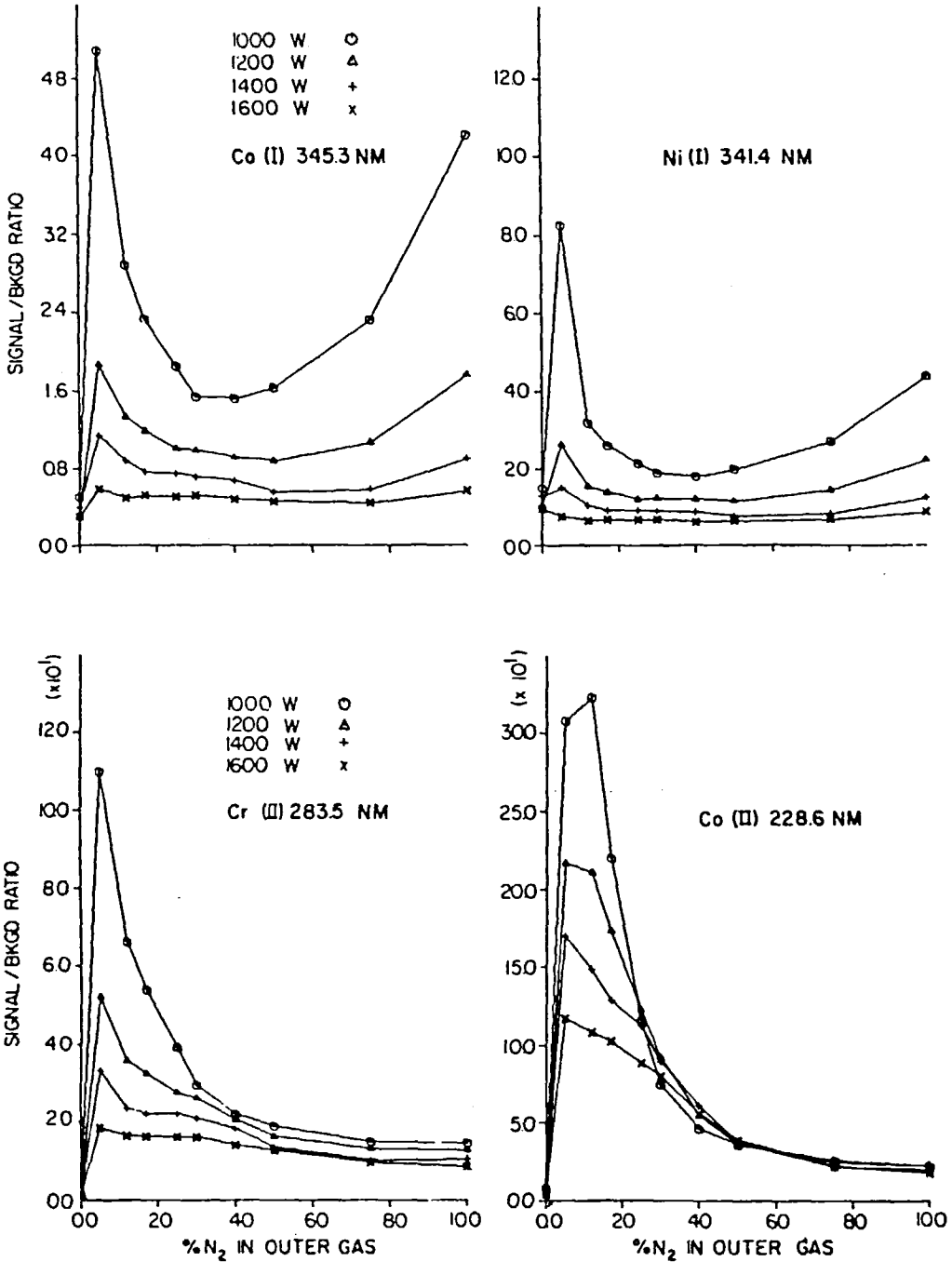

FIGURE 9. Effect of forward power and percent nitrogen in the outer flow on the S/B ratios of various atomic and ionic spectral lines. (From Montaser, A., Fassel, V. A., and Zalewski, J., *Appl. Spectrosc.*, 35, 292, 1981. With permission.)

power and a higher injector gas flow rate were required to observe the Ca I 422.6 vs. the Ca II 393.3-nm line.[26] Before a definite conclusion on the suitability of an air injector gas in an Ar-supported ICP can be made, further studies are required to examine the influence of air on the S/B and detection limits of a representative set of elements. Such studies are important for the direct injection of powders and aerosol of

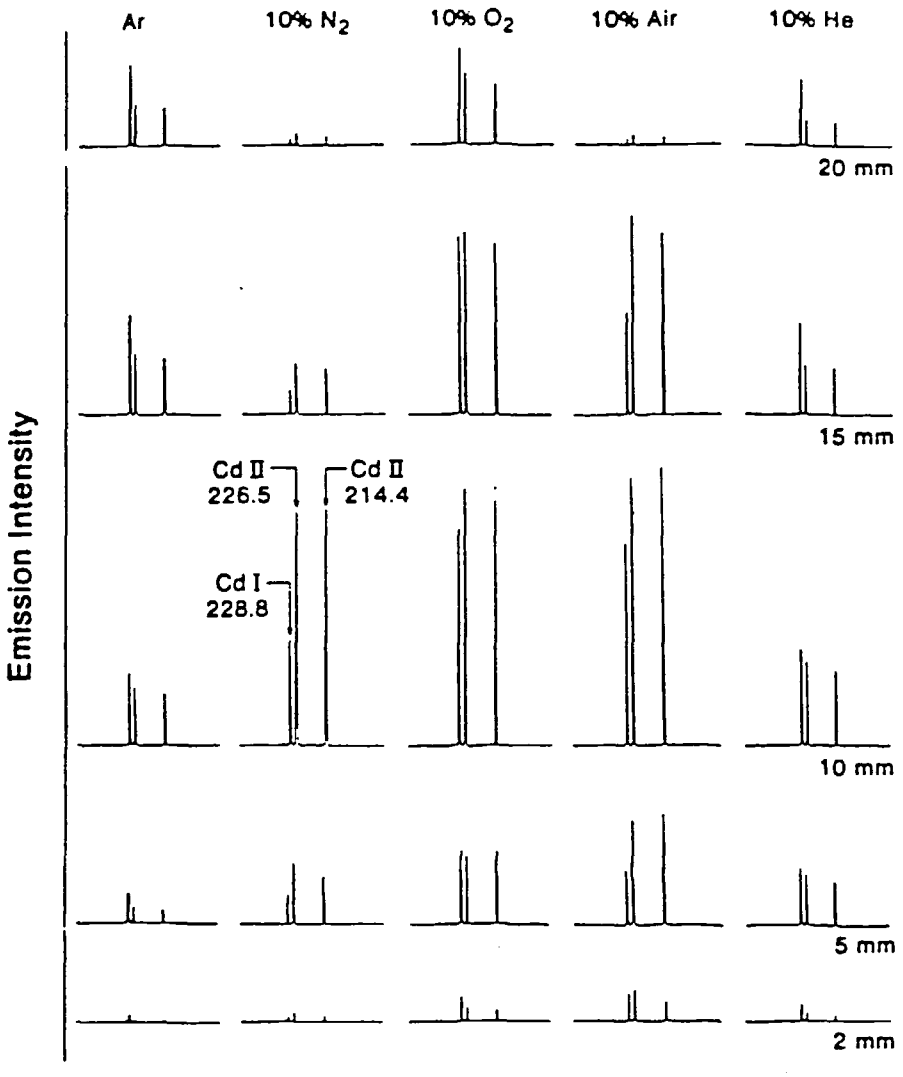

FIGURE 10. Comparison of Ar, Ar-N_2, Ar-O_2, Ar-air, and Ar-He ICPs for the measurement of cadmium hard lines. The nonargon plasmas contain 10% molecular gas or helium and 90% Ar in the outer gas flow. (From Choot, E. H. and Horlick, G., *Spectrochim. Acta*, 41B, 907, 1986. With permission.)

solid samples into an ICP discharge.[26] Studies are also required to explain why the S/B ratio of the Ca I line was reduced when the pneumatic nebulizer was replaced with an ultrasonic nebulizer by Meyer and Barnes.[26]

The influence of injector gas flows on the optimal operation of both molecular-gas plasmas and mixed-gas discharges, especially those with pure molecular gas in the outer flow, is quite significant. Thus, the optimum injector gas flows of Ar-N_2 plasmas[41,57,60,61,104] are generally greater than those used in Ar ICP. As the injector gas flow rate is increased from 1 to 2 *l*/min of Ar, the S/B ratios of certain spectral lines increased by a factor of 100 (Figure 11), for the Ar-N_2 ICP discharge formed in the Fassel torch.[57] Similarly, Meyer and Barnes noted that the optimum injector gas flow for the air ICP was greater than that for the N_2 ICP.[26]

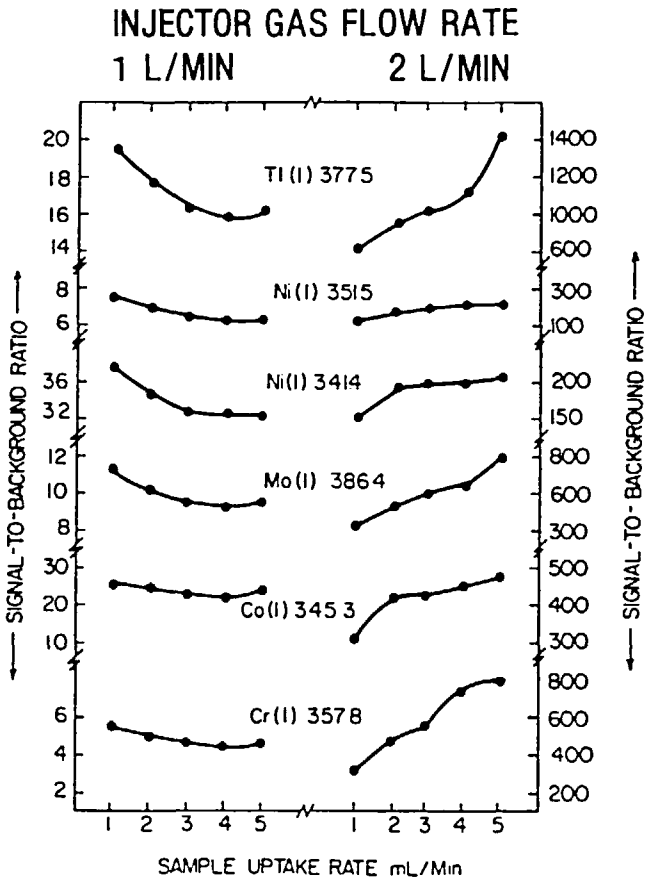

FIGURE 11. Influence of injector flow rate and sample uptake rate on S/B ratios of various elements in an Ar-N_2 plasma with pure nitrogen outer flow in a Fassel-type torch. (From Montaser, A., Fassel, V. A., and Zalewski, J., *Appl. Spectrosc.*, 35, 292, 1981. With permission.)

C. Selection of Operating Conditions

1. General Trends

For any ICP discharge, selection of optimum operating conditions for a particular sample depends on the type of torch used, the choice of spectral lines, and the generator frequency. In general, the forward power required to observe hard lines is higher than that used for monitoring soft lines. The power requirement is reduced, especially for molecular-gas ICP discharges, at higher generator frequencies.[68] Relatedly, higher gas flow and higher power are required to sustain the mixed- and molecular-gas plasmas in the Greenfield torch as compared to the Fassel torch and the low-gas-flow torches (Tables 1 to 3).

To reduce power and gas requirements of the ICP discharges formed in the Greenfield torch, Ebdon and associates[50] modified internal dimensions of the Greenfield torch and used simplex optimization to identify the optimized operating conditions of Ar and Ar-N_2 ICP discharges when Mn II 257.6-nm line was observed. Because these investigators[50] monitored a relatively large section of plasma tail flame (16 mm) and used an rf generator that could not deliver high enough power suitable for the Ar-N_2 ICP, no definite statements can be made at the present time on optimized operating conditions of the Ar-N_2 plasma formed in the modified Greenfield torch or the relative magnitude of the S/B ratios attainable in Ar and Ar-N_2 ICP discharges used in this

Table 6
OPTIMUM OPERATING CONDITIONS FOR MAXIMUM S/B RATIO IN SINGLE- AND MULTIPLE-ELEMENT DETERMINATIONS WITH AN Ar-N_2 ICP FORMED IN THE GREENFIELD TORCH

Element	Wavelength (nm)	Power (kW)	Intermediate gas flow (*l*/min)	Injector gas flow (*l*/min)	Observation height* (mm)
S I	182.0	6.4	22	1.6	7
As I	197.1	5.5	17	1.5	7
Zn I	213.8	6.0	19	1.7	8
P I	214.9	6.1	21	1.5	8
B I	249.7	5.8	17	1.5	7
Si I	251.6	3.1	16	1.4	7
Pt I	265.9	2.9	14	1.5	6
Au I	267.5	3.1	14	1.6	8
Al I	308.2	2.4	10	1.6	9
Cu I	324.7	2.6	12	1.3	7
Ag I	328.0	2.5	10	1.5	9
Sn II	189.9	4.7	17	1.4	6
Pb II	220.3	4.6	17	1.4	7
Ni II	231.6	5.1	17	1.4	8
Co II	238.8	4.9	17	1.5	8
Ta II	240.0	4.7	17	1.5	7
Mn II	257.6	4.2	16	1.4	7
Fe II	259.9	3.7	19	1.5	7
Mg II	279.5	4.6	17	1.5	8
Cr II	283.5	4.7	14	1.5	7
Nb II	309.4	3.4	19	1.4	7
Ca II	317.9	3.4	17	1.5	7
Ti II	337.2	4.2	19	1.4	7
Conditions for multiple-element analysis		4.8	17	1.5	7

* Measured from the top of the load coil.

From Moore, G. L., Humphries-Cuff, P. J., and Watson, A. E., *Spectrochim. Acta*, 39B, 915, 1984. With permission.

study. However, based on other studies,[57,60,62-64,104] certain general guidelines can be followed in selecting operating conditions of the Ar-N_2 plasmas generated in the Greenfield and Fassel torches. These trends, discussed below, should be applicable also to Ar-air and Ar-O_2 ICP discharges.

With respect to torch configuration, one should differenciate between the Ar-N_2 ICP discharges generated in the Greenfield[104] and Fassel torches.[57,60,62-64] Depending on the forward power utilized, both plasmas operate with outer gas flow of 15 to 40 *l*/min of N_2, but the optimum intermediate gas flow[104] for the Ar-N_2 ICP in the Greenfield torch varies (Table 6) between 10 to 22 *l*/min of Ar, a value much higher than the 1.5 to 2.5 *l*/min of Ar used in the Fassel torch for the Ar-N_2 ICP.[57,60,62-64] Thus, in terms of total Ar gas consumption, the Ar-N_2 ICP in the Greenfield torch resembles an Ar ICP discharge surrounded by an outer jacket of N_2. However, in contrast to the commonly used Ar ICP in the Fassel torch, typically operated at 1.2 kW and 15 mm observation height, the Ar-N_2 ICP in the Greenfield torch must be observed at 4.7 kW and 7 mm for simultaneous multielement analysis.[104] Apparently, the diffusion of N_2 from the

outer gas flow into the axial channel changes the operating conditions significantly, although the analytical performance of Ar-N_2 ICP[104] in the Greenfield torch and the Ar ICP discharge[28] in the Fassel torch are comparable, especially when hard lines are used. In contrast, the detection power of an Ar-N_2 ICP in the Fassel torch[57] operated at 2.0 to 3.5 kW only approaches that of the commonly used Ar ICP[28] when hard lines are used. In principle, the use of higher power should improve the detection limits the Ar-N_2 plasma even further, but at powers >3.5 kW, the Ar-N_2 ICP in the Fassel torch assumes[57] the shape of an "inverted cone" (Figure 1e). For the inverted-cone shape, the analyte emission is not limited to the axial channel, but is distributed throughout the inverted cone, thus reducing the number of emitting species per unit volume. If soft lines are used to monitor the plasmas, then the Ar-N_2 ICP formed in the Fassel torch may be operated at the same power level and observation height of the commonly used Ar ICP,[28] but the detection limits of many elements are superior[57,60] to the best results achieved for the Ar ICP discharge. This observation about soft lines has also been confirmed for the Ar-N_2 ICP generated in the Greenfield torch.[41,104]

2. Empirical Correlations Between Excitation Properties of Elements and Optimum Parameters of ICP Discharges

The above discussion on Ar and Ar-N_2 ICP discharges suggests the existance of certain empirical correlations between the optimum parameters and the excitation properties of elements in ICP discharges. For the Ar-N_2 plasma formed in the Greenfield torch, the possible relation between the power required for the maximum S/B ratio to be achieved for each element and the difficulty of excitation has been explored by plotting the optimum power vs. the ionization potentials of the species investigated.[41,104] The best correlation has been established[104] to occur when the first ionization potentials of the soft atomic lines and the second ionization potentials of the hard atomic and ionic lines were used (Figure 12). The extent of the existence of a relation between the optimum power for maximum S/B ratio and the corresponding optimum intermediate gas flow is shown in Figure 13 for the Ar-N_2 ICP in the Greenfield torch.[104] While the soft lines require lower power and a lower intermediate-gas-flow rate, the opposite trend is observed for the hard lines. For the Ar-N_2 plasma in the Fassel torch, a small range of intermediate-gas flows (1.5 to 2.5 *l*/min of Ar) have been used, but the correlation between optimum power and the difficulty for excitation of soft and hard lines has also been established.[57] The possible existence of the relation between outer gas composition in an Ar-N_2 ICP[57] and the behavior of the soft and hard lines was documented in Figure 9 and discussed in Section IV.B. A similar correlation has been noted for Ar-H_2 ICP[34] using 6.5% H_2 in the various flows of an Ar ICP (Figure 14). Because of the presence of H_2, the net intensity of many elements, especially hard ion and atom lines in the wavelength range of 200 to 300 nm, were increased, thereby improving the detection limits.[34,35,81] Studies of Choot and Horlick[62-64] on Ar-N_2, Ar-O_2, and Ar-air ICP discharges have also documented the disparity of the behavior of Ca 393.4 nm, and the Cd lines from 214 to 228 nm, especially when the outer flow contained 100% molecular gas.

The trends in the behavior of spectral lines have also been studied by Meyer et al.[26,68] for molecular-gas plasmas. The spatial distributions of atomic transitions within the tailflame of air and O_2 ICP discharges (Figure 15), indicate that, similar to the behavior reported for an Ar ICP,[109] spectral lines having high excitation energies should be monitored at observation heights higher than those possessing low excitation potentials.[68] Relatedly, atomic emission lines of high excitation energies were located radially further from the center line of the air ICP discharge.[68] In contrast, no empirical correlation was noted between the excitation potential of ionic transitions and their spatial distribution within the air and O_2 plasmas[68] (Figure 16).

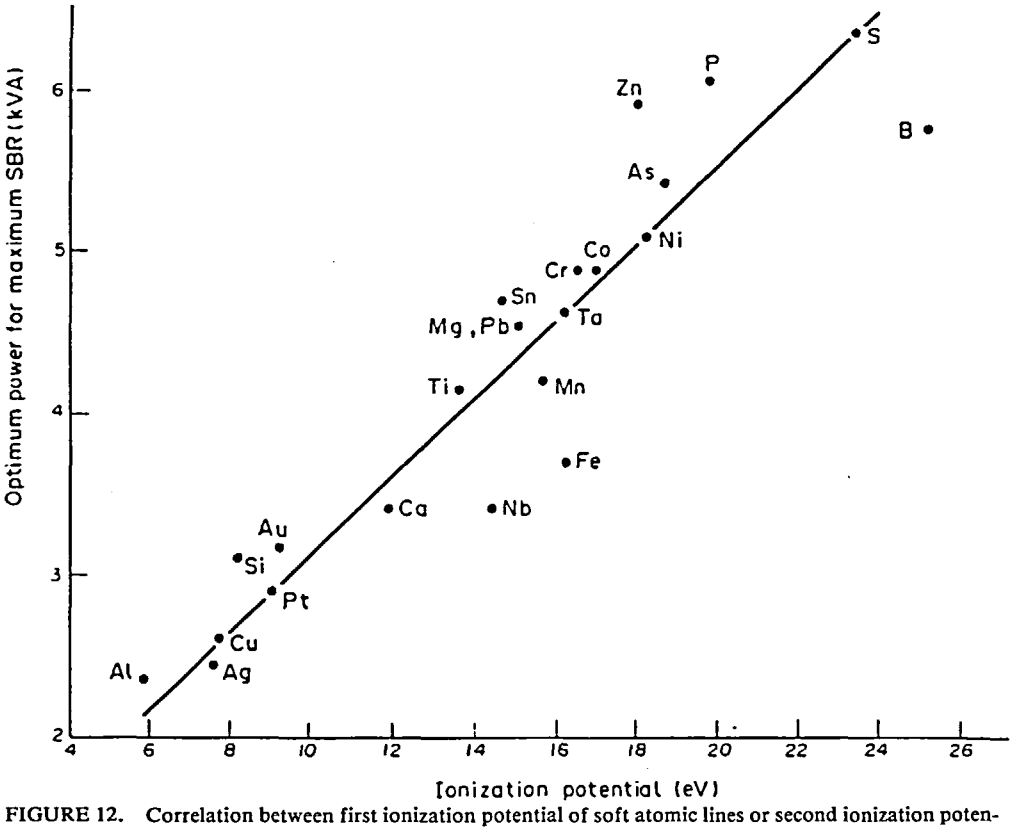

FIGURE 12. Correlation between first ionization potential of soft atomic lines or second ionization potential of hard lines and optimum rf power for maximum S/B ratio achieved in an Ar-N_2 plasma generated in Greenfield-type torch. (From Moore, G. L., Humphries-Cuff, P. J., and Watson, A. E., *Spectrochim. Acta, 39B, 915, 1984.* With permission.)

The above discussion clearly reveals that, as expected, the difficulty of exciting a particular spectral line in any plasma exhibits a correlation with the energy available in various species in the discharge: the higher the energy, the greater the efficiency of the excitation process. Thus, for those elements which are difficult to excite, such as the halogens, the He ICP discharges should be the most efficient excitation source.[75-77] The best criterion for comparing the efficiencies of plasmas in exciting atomic emission is population density maps of analyte in ground and excited states. When such maps are not available for all the ICP discharges, comparison of the detection limits, obtained under optimized conditions, is the best *practical* criterion for evaluating the excitation efficiencies of the plasmas.

D. Detection Limits

Because a variety of equipment and operating conditions are used, intercomparison of detection limits achievable with ICP discharges should be done with extreme caution, especially when detection limits are not reported for simplex-optimized conditions or when the IUPAC definition is not used by all investigators for calculations of detection limits. Relatedly, because of the disparity between the background spectra emitted by the various ICP discharges, the limits of determinations may be inferior, sometimes by two orders of magnitude, compared to the detection limits.[105] Another difficulty arises when, within a period of approximately 5 years, the same investigators report different sets of detection limits for the same set of elements, excited in the same ICP. To cite a typical example, detection limits obtained by Ohls and Sommer during the

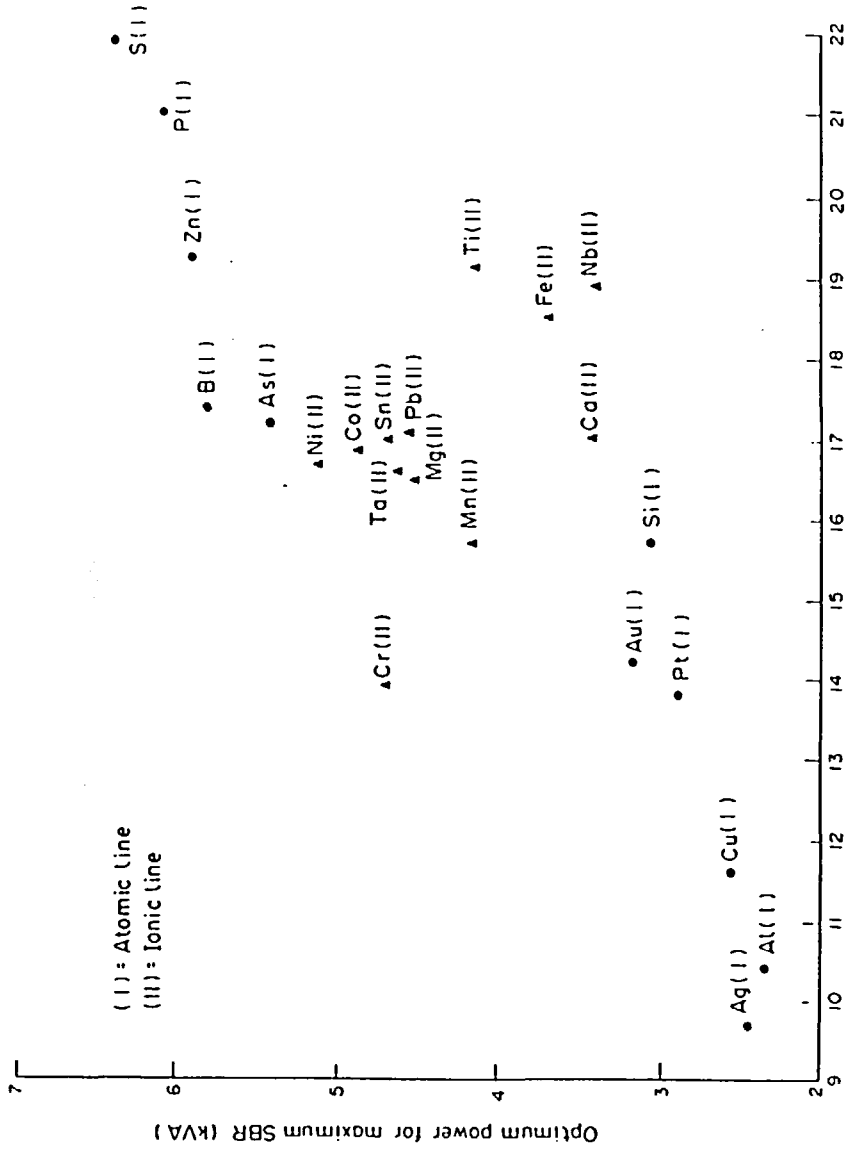

FIGURE 13. Correlation between optimum rf power and optimum intermediate gas flow rate for maximum S/B in an Ar-N_2 plasma generated in a Greenfield-type torch. (From Moore, G. L., Humphries-Cuff, P. J., and Watson, A. E., *Spectrochim. Acta*, 39B, 1984. With permission.)

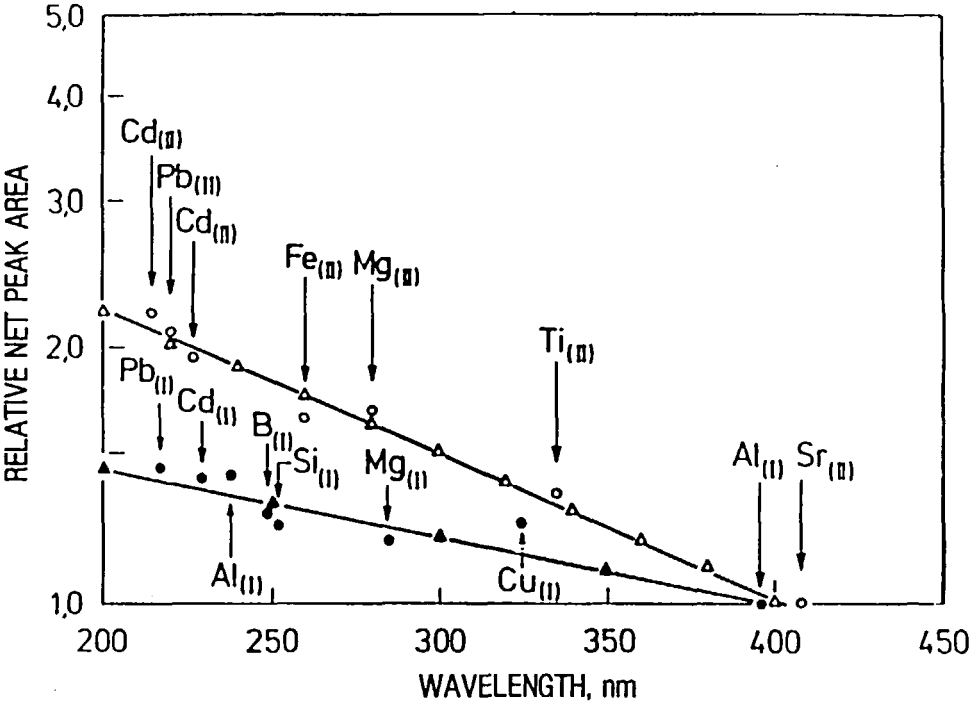

FIGURE 14. Correlation between intensity and the difficulty of excitation of atom and ion lines for an Ar-H_2 plasma with 6.5% H_2 in the outer flow. (From Schramel, P., Fisher, R., Wolf, A., and Hasse, S., *ICP Inform. Newsl.*, 6, 401, 1981. With permission.)

period of 1979 to 1984 are compiled in Table 7 for an Ar-N_2 ICP generated in the Greenfield torch.[51,55,56] The operating conditions for the plasmas and the reciprocal linear dispersion of the spectrometers used are also listed in the table. The detection limits reported in 1984[55] are inferior, by a factor of 100 for certain elements, to the previous results[51,56] reported by the same investigators. Although no explanation is provided by the authors, a comparison of the operating conditions shows that a very low injector gas flow was used for the measurements in 1984.[55] The use of such a low injector gas flow is quite uncommon for the Ar-N_2 ICP discharge, as many investigators have shown that the injector gas flows of an Ar-N_2 plasma generated in both the Greenfield[41,45,49,104] and Fassel[57,60,62-64] torches are higher than the value used in Ar ICP discharge.

The most comprehensive compilation of detection limits for an Ar-N_2 ICP generated in the Greenfield torch under optimized conditions is reported by Moore et al.[104] (Table 8). For comparison, the detection limits reported for Ar-O_2 ICP[55] and Ar-air ICP,[56] generated in the Greenfield torch, and the detection limits for the commonly used Ar ICP,[28] formed in the Fassel torch are also listed in Table 8. Two conclusions may be drawn from the data in Table 8. First, at a forward power of 4.75 kW, the detection limits for an Ar-N_2 ICP approach those for a 1.1-kW Ar ICP. Second, for the limited number of elements tested, the Ar-O_2 plasma,[55] operated at 2.8 kW, generally provided inferior detection limits than other plasmas. The use of forward power > 3 kW may improve the detection limits obtained in both the Ar-O_2 and Ar-air ICPs. Experimental verification of this prediction is important because both Ar-O_2 and Ar-air ICP discharges are particularly useful when the sample contains a large concentration of organic substances. Of course, because of spectral interferences from CN and CO

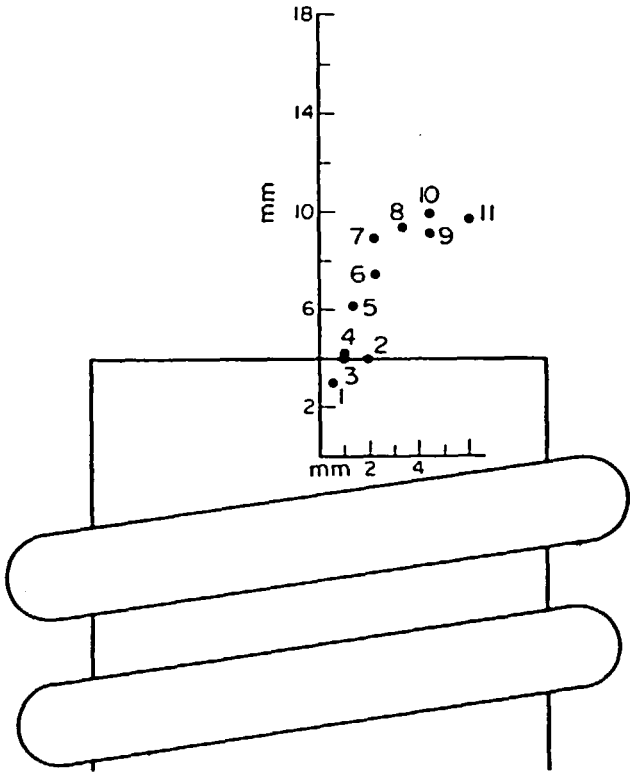

A

FIGURE 15. Spatial distribution of atomic emission lines in air (A) and O_2 ICPs (B) generated in demountable torch. [ ], excitation potentials in eV. (A): 1, K [1.6]; 2, Ca [2.9]; 3, Li [1.8]; 4, Ga [3.1]; 5, Mg [5.9]; 6, Mn; 7, Al [5.2]; 8, Pd; 9, Zn [5.8]; 10, Cd [5.4]; 11, Be [5.4]; and (B): 1, Na [2.1]; 2, Zn [5.8]; 3, Ca [2.9]; 4, Pd; 5, Mg [5.9]; 6, Mn; 7, Al [5.2]; 8, Li [3.8]; 9, Ga [4.3]; 10, Cd [5.4]; 11, Be [5.4]. (From Meyer, G. A. and Thompson, M. D., *Spectrochim. Acta*, 40B, 195, 1985. With permission.)

bands,[91] the choice of a plasma for organic sample analysis is dependent on the spectral line monitered.

The detection limits listed in Table 8 were obtained for mixed-gas plasmas generated in the Greenfield torch. For the Fassel torch, there are no reports for Ar-O_2 and Ar-air plasmas, but the comprehensive studies of Montaser et al.[57] show that even at 3.0 to 3.5 kW, the detection limits of hard lines excited in an Ar-N_2 ICP with a pure nitrogen outer flow are inferior to those from the commonly used Ar ICP discharge generated at 1.0 to 1.2 kW.[28] As discussed in Section IV.C, rf power > 3.5 kW may not be used for the Ar-N_2 plasma in the Fassel torch because the plasma assumes the shape of an inverted cone. In contrast, if soft lines are used to observe the Ar-N_2 plasma,[60] the detection limits (Table 9), obtained in the Ar-N_2 ICP are superior or equivalent to the best results achieved for the Ar ICP discharge.[28] Observation of soft lines allows operation of Ar-N_2 ICP at conditions commonly used for Ar ICP, i.e., 1.2-kW forward power, 15-mm observation height, and 20-*l*/min total gas flow.

With reference to Ar-H_2 ICP discharge, studies of Schramel et al.[34,35,81] seem to indicate that addition of small amounts of hydrogen to various gas flows of an Ar

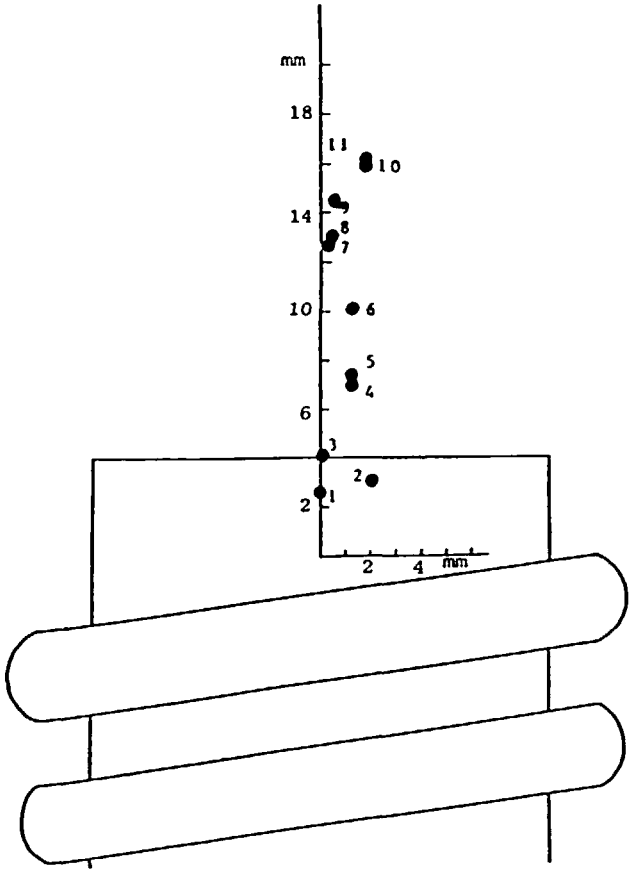

FIGURE 15B.

ICP, especially the intermediate gas flow,[35] tend to improve the detection limits of elements by a factor of 2 to 3, in particular, those measured for the hard lines. Because studies of the Ar-H_2 plasma[35] have been conducted over a narrow range of experimental conditions, for example, the power was changed between 750 to 1050 W and the outer gas flow contained a maximum of only 6.5% H_2, a definite conclusion on the analytical utility of the Ar-H_2 ICP discharge may not be made at the present time.

For molecular-gas ICP discharges, detection limits have been obtained at 41 MHz and 1.5 to 2.0 kW[68] (Table 10), and at 27 MHz and 3.5 to 4.0 kW (Table 11).[26] Two conclusions may be drawn from the data in the tables. First, for most elements, the detection limits obtained in the molecular-gas plasmas are 2 to 100 times inferior[26,68] to the results achieved for the Ar ICP discharge. Second, compared to molecular-gas plasmas, the air ICP provides lower detection limits, especially for spectral lines of long wavelengths such as the alkali metals.[26] Importantly, the detection limits reported for the air ICP discharge at 41 MHz and 1.5 to 2.0 kW[68] are inferior to those reported for the same plasma at 27 MHz and 3.5 to 4.0 kW.[26] Since different spectrometers were used to obtain the data in Tables 10 and 11 for the air ICP, no definite conclusion on the influence of frequency and rf power on the detection limits can be stated at the present time. However, the results in Tables 10 and 11 seem to indicate that some Ar is required in the plasmas, as in the Ar-N_2,[60,104] to achieve detection limits similar to those for an Ar ICP discharge, especially when spectral lines of high excitation energies are used to observe the plasmas.

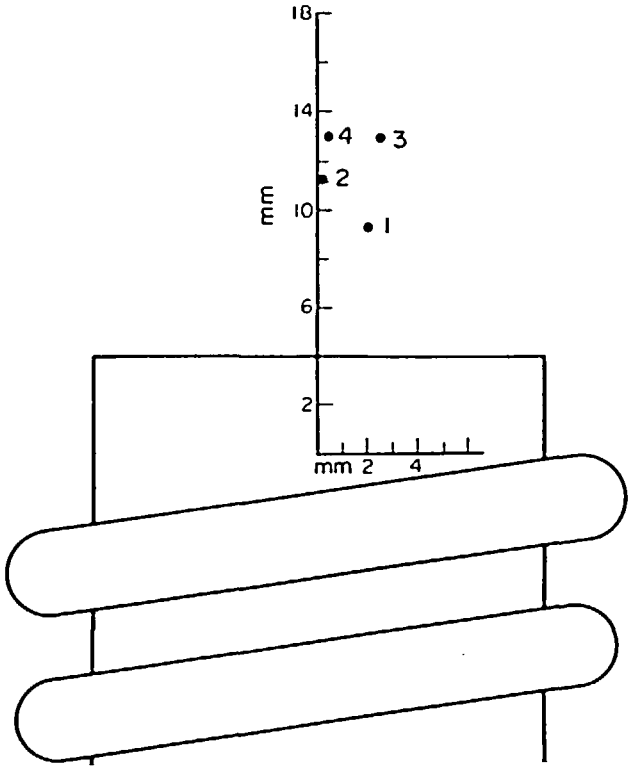

FIGURE 16. Spatial distribution of ionic emission lines in air (A) and O_2 ICPs (B) generated in demountable torch; [ ], excitation potential in eV. (A): 1, Mn; 2, Nb; 3, Ti [11.1]; 4, La [9.1]; 5, Mg [12.0]; 6, Be [13.2]; 7, Ca [9.2]; 8, Cd [14.2]; 9, Ba [7.9]; 10, Pd [16.3]; and (B): 1, Mg [12.0]; 2, Ca [9.2]; 3, Be [13.2]; 4, Ba [7.9]. (From Meyer, G. A. and Thompson, M. D., *Spectrochim. Acta*, 40B, 195, 1985. With permission.)

In principle, for difficult-to-excite lines, the He-ICP discharges[73-77] should be the most viable source. The results in Table 12 show that the detection limits Cl and Br in the annular He ICP are superior to those obtained for an Ar plasma by factors of 65 and 33, respectively.

Aside from detection limits, one should explore whether mixed-gas, molecular-gas, and He ICP discharges exhibit the relative freedom from interferences noted for the Ar plasma. This subject is discussed in the following section.

E. Chemical Interferences and Analytical Applications

Except for the Ar ICP, the mixed-gas plasmas, and in particular, the Ar-N_2 ICP, have been investigated to a greater extent in terms of relative freedom from physical and chemical interferences. Relatedly, many applications of the Ar-N_2 ICP to the elemental analysis of a variety of substances, including standard reference materials, have appeared in the literature (Table 13). These applications document the relative freedom of mixed-gas plasmas from solute vaporization-atomization interferences. Because of their high temperatures, Section V.A.3, similar freedom from interference is expected for molecular-gas ICPs, although such studies have not yet been reported. The capa-

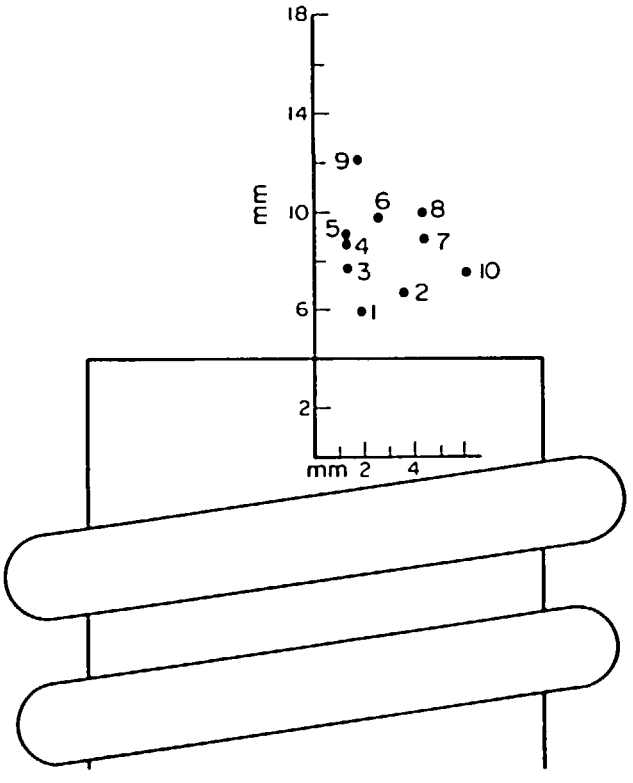

FIGURE 16B.

bility of the He ICP discharges in handling complex matrices also remains to be investigated.

The extent of the solute vaporization-atomization interferences and the effect of easily ionized elements (EIE) depend on the composition of the outer gas in the mixed-gas ICP, the observation height, and the forward power. Thus, as the percent nitrogen or oxygen was increased from 0 to 100% in the outer flow of Ar-N_2 and Ar-O_2 plasmas, respectively, both interferences were reduced[61,64] substantially, especially when the observation height was increased from 2 to 18 mm above the load coil for a Fassel torch operated at about 2 kW. Even at the lower rf power of 1.2 kW, no solute vaporization-atomization interferences were reported by Montaser et al.,[60] but EIE enhanced emission of soft atom lines excited in the Ar-N_2 ICP operated in the Fassel torch.

Studies of the effect of EIE on the net analyte intensities, observed from an Ar-N_2 plasma generated in the Greenfield torch, show that even at powers around 5 kW, ion line depression and atom line enhancement are observed (Table 14) if the analyst desires to achieve maximum S/B ratios in multielement analysis.[104] Ionization interference to less than 5% levels may be achieved if lower S/B ratios are accepted.[104]

The best criterion for evaluating matrix interferences is chemical analysis of standard reference materials. The plots[49,86] shown in Figures 17 and 18 clearly demonstrate the capability of mixed-gas plasmas in the analysis of complex substances. In this respect, the precision and accuracy of such determinations are comparable to Ar ICP discharges, with the added advantage that mixed-gas and molecular-gas plasmas, because of the use of higher power, are more robust. Chemical interferences in Ar-air, Ar-He, and Ar-H_2 plasmas generated in either a Greenfield torch, a Fassel torch, or a low-gas-flow torch need to be investigated to comprehensively compare the relative analytical capabilities of various mixed-gas plasmas.

Table 7
DETECTION LIMITS REPORTED BY OHLS AND SOMMER[51,55,56] FOR AN Ar-N_2 ICP GENERATED IN THE GREENFIELD TORCH

Element	Wavelength (nm)	Detection limit* 1979 (ng/g)	1981 (ng/ml)	1984 (ng/g)
B I	208.9	40.0	4.0	300.0
Zn I	213.8	40.0	1.0	13.0
Pb II	220.3	400.0	5.0	120.0
Ni II	231.6	200.0	6.0	40.0
B I	249.6	0.6	7.0	7.0
Mn II	257.6	1.0	0.3	—
Mg II	279.5	0.06	0.5	0.4
Si I	288.1	300.0	3.0	—
Cu I	324.7	300.0	3.0	25.0
Ca II	393.3	0.02	0.4	—
rf power, kW		3.0	3.0	2.8
Observation height, mm		8.0	8.0	8.0
Outer gas flow, l/min of N_2		28.0	27.0	16.0
Intermediate gas flow, l/min of Ar		15.0	11.0	9.0
Injector gas flow, l/min of Ar		1.0	1.0	0.3—0.4
Sample uptake rate, ml/min		2.0	3.2	—
Nebulizer type		Concentric	Crossflow	Concentric
Reciprocal linear dispersion, nm/mm		1.2	0.46	0.46

* Results are for aqueous solutions; the same rf generator is used in all experiments.

V. PLASMA DIAGNOSTICS

The most important criteria used to access fundamental properties of analytical ICPs are temperatures and electron number densities. These properties can provide insight on the various reaction mechanisms prevailing in the plasmas, the extent of departure from local thermodynamic equilibrium, and the role of different species in exciting the analyte. Relatively few investigators have reported the temperature or electron number density for their plasmas. Molecular-gas plasmas have been characterized to a greater extent than other nonargon discharges. In this section, the available data on temperature and electron number density are summarized to illustrate gaps of such data for various ICP discharges. In addition, recent work on computer modeling of plasmas is briefly discussed.

A. Temperature Measurements

1. ICP Discharges with Alternate Injector Gases

Alder and Mermet[32] measured rotational temperatures in an argon-methane ICP by recording the intensities of P branch lines of the (0—0) Swan band system of C_2. As shown in Table 15, the rotational temperature (6100 K) measured immediately above the coil was comparable to the excitation temperatures measured for Ar I lines. At higher observation heights, the excitation temperature was reduced. Thus, for exam-

Table 8
DETECTION LIMITS (ng/m*l*) OBTAINED FOR MIXED-GAS ICPs

Element, spectrum	Wavelength (nm)	Ar[28]	Ar-N_2[104]	Ar-O_2[55]	Ar-air[56]
Sn II	189.9	25.0	70.0		
As I	197.1	76.0	140.0	150.0	
Zn I	213.8	1.8	14.0	13.0	8.0
P I	214.9	76.0	130.0		
Pb II	220.3	42.0	97.0	160.0	
Ni II	231.6	15.0	16.0	30.0	80.0
Co II	238.8	6.0	9.4		
Ta II	240.0	28.0	33.0		
B I	249.7	4.8	5.3	20.0	0.7
Si I	251.6	12.0	25.0		
Mn II	257.6	1.4	1.0		8.0
Fe II	259.9	6.2	6.2	6.0	
Pt I	265.9	81.0	57.0		
Au I	267.5	31.0	16.0		
Mg II	279.5	0.2	2.5	0.1	0.01
Cr II	283.5	7.1	4.5		
Al I	308.2	45.0	81.0		
Ca II	317.9	10.0	25.0		
Cu I	324.7	5.4	7.5	13.0	6.0
RF power, kW		1.1	4.8	2.8	3.0
Observation height, mm		12—18	7.0	8.0	8.0
Outer gas flow, *l*/min		20 Ar	23 N_2	16 O_2	28 air
Intermediate gas flow, *l*/min of Ar		0	17.0	9.0	15.0
Injector gas flow, *l*/min of Ar		1.0	1.5	0.3—0.4	1.0

Table 9
S/B RATIOS AND ESTIMATED DETECTION LIMITS (ng/m*l*) FOR THE RELATIVELY LOW-POWER Ar-N_2 ICP[a60] AND THE Ar ICP[b]

Element	Concentration (μg/m*l*)	S/B ratios: Ar-N_2 ICP	S/B ratios: Ar ICP	Detection limit: Ar-N_2 ICP	Detection limit: Ar ICP	Improvement factor
Li I 670.7	0.1	230.0	0.8[c]	0.013	3.8	290.0
Na I 588.9	1.0	100.0	1.0	0.30	29.0	100.0
Rb I 780.0	100.0	200.0	2.5[c]	15.0	1200.0	80.0
Ga I 417.2	1.0	43.0	0.64 (I 294.3)	0.70	46.0	67.0
Al I 396.1	1.0	78.0	1.3 (I 309.2)	0.38	23.0	60.0
Rh I 369.2	1.0	32.0	0.67 (II 233.4)	0.94	44.0	48.0
Ru I 372.8	1.0	25.0	1.0 (II 240.2)	1.2	30.0	25.0
In I 451.1	10.0	85.0	4.7 (II 230.6)	3.5	63.0	18.0
U II 385.9	10.0	15.0	1.2	20.0	250.0	13.0
Cr I 357.8	1.0	57.0	4.9 (II 205.5)	0.53	6.1	12.0
Dy II 353.1	1.0	35.0	3.0	0.86	10.0	12.0
Tl I 377.5	10.0	87.0	7.4 (II 190.8)	3.4	40.0	12.0
Mo I 386.4	1.0	37.0	3.8 (II 202.0)	0.81	7.9	10.0
Sm II 359.2	10.0	69.0	6.9	4.3	43.0	10.0
Er II 390.6	1.0	26.0	2.9 (II 337.2)	1.2	10.0	9.0
Ba II 455.4	1.0	210.0	23.0	0.14	1.3	9.0

Table 9 (continued)
S/B RATIOS AND ESTIMATED DETECTION LIMITS (ng/mℓ) FOR THE RELATIVELY LOW-POWER Ar-N_2 ICP[a60] AND THE Ar ICP[b]

Cu I 324.7	1.0	47.0	5.6	0.64	5.4	8.0
Nd II 401.2	10.0	46.0	5.9	6.5	50.0	8.0
Eu II 381.9	1.0	90.0	11.0	0.33	2.7	8.0
Tm II 384.8	1.0	38.0	5.8 (II 313.1)	0.79	5.2	7.0
Ho II 345.6	1.0	31.0	5.3	0.97	5.7	6.0
Tb II 350.9	1.0	8.2	1.3	3.7	23.0	6.0
Y II 377.4	1.0	42.0	8.6 (II 371.0)	0.71	3.5	5.0
Yb II 369.4	1.0	90.0	17.0 (II 328.9)	0.33	1.8	5.0
Pb I 405.7	100.0	300.0	70.0 (II 220.3)	10.0	42.0	4.0
Sc II 361.3	1.0	85.0	20.0	0.35	1.5	4.0
La II 408.6	1.0	10.0	3.0	3.0	10.0	3.0
Pr II 390.8	10.0	21.0	8.1	14.0	37.0	3.0
Ca II 393.3	0.5	240.0	89.0	0.063	0.17	3.0
Sr II 407.7	0.5	120.0	36.0	0.13	0.42	3.0
Th II 401.9	10.0	14.0	4.6 (II 283.7)	21.0	65.0	3.0
V I 437.9	10.0	170.0	60.0 (II 309.3)	1.8	5.0	3.0
Ce II 413.7	10.0	16.0	6.2	19.0	48.0	3.0
Ag I 328.0	10.0	75.0	38.0	4.0	7.9	2.0
Fe I 371.9	10.0	100.0	65.0 (II 238.2)	3.0	4.6	2.0
Mn I 403.3	1.0	36.0	22.0 (II 257.6)	0.83	1.4	2.0
Nb I 407.9	10.0	20.0	8.3 (II 309.4)	15.0	36.0	2.0
Ni I 351.5	10.0	65.0	29.0 (II 221.6)	4.6	10.0	2.0
Zr II 343.8	1.0	6.6	4.2	4.5	7.1	2.0
Co I 345.3	10.0	55.0	50.0 (II 238.8)	5.5	6.0	1.0
Sn I 303.4	100.0	55.0	120.0 (II 189.9)	55.0	25.0	0.5
B I 249.7	10.0	5.5	63.0	55.0	4.8	0.1
Sb I 259.8	100.0	12.0	91.0 (I 206.8)	250.0	32.0	0.1
Bi I 306.7	100.0	10.0	87.0 (I 223.0)	300.0	34.0	0.1
Cd I 361.0	10.0	15.0	120.0 (II 214.4)	20.0	2.5	0.1

[a] Operating conditions: outer flow rate, 15 ℓ/min of N_2; intermediate flow rate, 2.5 ℓ/min of Ar; injector gas flow rate, 2.5 ℓ/min of Ar corresponding to a 60 psi nebulizer pressure; sample uptake rate, 3.5 mℓ/min; forward power, 1.2 kW; observation height, 20 mm.

[b] From Reference 28.

[c] Measured in this work under the commonly used experimental conditions: outer flow rate, 20 ℓ/min of Ar; injector gas flow rate, 1 ℓ/min of Ar; sample uptake rate, 1.9 mℓ/min; forward power, 1.1 kW; observation zone, 12 to 18 mm.[28]

Table 10
DETECTION LIMITS (μg/mℓ) FOR AIR AND O_2 ICPs OPERATED AT 41 MHz AND 1.5 TO 2.0 kW.[68]

Element	Wavelength (nm)	Argon	Air	Oxygen	Air/Ar	Oxygen/Ar
Zn I	213.8	0.065	0.71	1.24	11.0	19.0
Cd II	214.4	0.09	61.7		685.0	
Cd II	226.5	0.11	36.6		332.0	
Pd II	229.6	2.2	15.5		7.0	
Be I	234.8	0.006	0.12	1.9	20.0	317.0
Pd II	236.7	17.8	25.0		1.0	
Pd II	248.8	1.8	8.3		5.0	
Mn II	257.6	0.0037	0.41		110.0	
Nb II	269.7	0.28	7.1		25.0	
Mn I	279.4	0.15	0.3		2.0	
Mg II	279.5	0.0007	0.4	2.5	571.0	3571.0

Table 10 (continued)
DETECTION LIMITS (μg/mℓ) FOR AIR AND O_2 ICPs OPERATED AT 41 MHz AND 1.5 TO 2.0 kW.[68]

Element	Wavelength (nm)	Argon	Air	Oxygen	Air/Ar	Oxygen/Ar
Mn I	280.1	0.22	0.55		3.0	
Mg II	285.2	0.0057	0.61		107.0	
Na I	285.3	200.0	14.9	3.7	0.08	0.02
Ga I	294.3	0.37	2.7	3.0	7.0	8.0
Nb II	309.4	0.11	1.1		10.0	
La II	333.7	0.043	0.89		21.0	
Ti II	334.9	0.017	0.11		6.0	
Ti II	338.3	0.019	0.11		7.0	
Pd I	363.4	0.19	0.18	0.81	1.0	4.0
Mg I	383.8	0.081	0.78	3.7	10.0	46.0
Ca II	393.3	0.0003	0.0008	0.021	3.0	70.0
La II	394.9	0.015	0.61		41.0	
Al I	396.1	0.057	0.12	0.40	2.0	7.0
Mn I	402.0	1.0	0.15		0.2	
Ga I	417.2	0.18	0.75	0.90	15.0	5.0
Ca I	422.6	0.017	0.023	0.17	1.0	10.0
La II	442.9	0.042	1.6		38.0	
Ba II	455.4	0.0012	0.012	0.026	10.0	22.0
Cd I	470.9	7.7	120.0		15.0	
Ba II	493.4	0.0018	0.012	0.051	7.0	28.0
Na I	588.9	0.065	0.059	0.19	1.0	3.0
Na I	589.5	0.025	0.076	0.35	3.0	14.0
Li I	610.3	0.12	0.8	10.7	7.0	89.0
Li I	670.7	0.16	0.16		1.0	
K I	766.4	0.41	0.96		2.0	
K I	769.9	0.89	3.8		4.0	
Rb I	780.0	1.4	14.5		10.0	
Rb I	794.7	0.19	22.1		116.0	

Table 11
DETECTION LIMITS (ng/mℓ) FOR AIR AND N_2 ICPs OPERATED AT 27 MHz AND 3.0 TO 4.4 kW.[26]

Element	Wavelength (nm)	Air	Nitrogen
Ca II	393.3	0.2	1.2
Al I	396.1	35.0	1500.0
Eu II	397.1	40.0	300.0
Mn I	403.0	27.0	3000.0
Na I	588.9	0.72	900.0
La I	624.9	800.0	7500.0

Table 12
ESTIMATED DETECTION LIMITS (μg/mℓ) OF Cl AND Br IN Ar ICP AND He ICP[75]

Element	Wavelength (nm)	Excitation energy (eV)	Annular He ICP	Ar ICP	Improvement* factor
Cl I	725.6	10.6	13	820	63
Br I	700.5	9.8	57	620	11
	734.8	9.7	18	620	34

* Improvement factor = DL in Ar ICP/DL in He ICP.

Table 13
APPLICATIONS OF MIXED-GAS AND MOLECULAR-GAS ICPs

Sample type	Elements	Matrix	Comments*	Ref.
Airborne particulates	Al, Ca, Cr, Cu, Fe, Mg, Mn, Ni, Pb, Sr, V, Zn	Atmospheric dusts and aerosols		93
Biological samples	Cr, Fe, Al, Cu, Mg, Si, Ag, Pb, P	Blood	Discrete (μl) sample introduction	39
	Al	Blood		60
Geological materials	Pb, Mg, Fe	Phosphate rocks		90
	Rare earths	Silicate and phosphate rocks		49
	Si, Al, Fe, Mg, Ca, Mn, Ti	Silicate and phosphate rocks		43
	Rare earths	Silicates, carbonates, and phosphates		48
	Rare earths	Apatite		47
	Rare earths	Silicates		110
	Sr, Ba, Ca	Celestite		38
	Numerous elements	Magnesite, phosphorus mud, celestite, etc.		6
	Nb, Sn, Ta	Pegmatite		104
	Numerous	Sulfides		111
Organics	Cd, Cu, Fe, Mn, Zn, Mg, Si, Co, Al, Pb, Cr	Lubricating oils, organic solvents, and waste waters	Metals were determined as APDTC complexes in MIBK	46
	Si, Pb	Petroleum, fuels	Gas chromatograph with ICP detection	52
	Cr, Fe, Al, Cu, Mg	Xylene, organometallics, oils and organic phosphates	Discrete (μl) sample introduction	39
	Cd	Petroleum, soils, plants, and fertilizers	Graphite cup sample introduction	112
	Sn	Hydrolic fluids	Hydride generation	113
	Cd, Mn, Pb, Zn	Soils, plants, and fertilizers	Electrothermal vaporization	114
Refractories and oxides	Be, B	Magnesium oxide	Direct powder injection	23
	V, Cu, Mn, Ni, Cr, As	CaO, alumina, Fe and titanium oxide	Direct powder injection	53
	Ca	Calcium carbonate, CaO	Direct powder injection into air ICP	26
Steels and ores	Ca	Iron or steel filings		51
	Pt, Pd, Ru, Rh, Au	Platinum ores and floatation feeds		94
	Numerous elements	Alloy steels, chrome ores		6
	Mn, Cr, Cu, Mo, Ni, V, Ti, Fe	Alloyed and unalloyed steels		54
	Cu	Bronzes and alloys		86
	Ce	Steels	Ar-O_2 ICP	55
	Sn	Iron and brass	Hydride generation	115
	15 elements	Aluminum		116
	Cu, Fe, Mg, Mn, Si	Aluminum alloys	Direct sample introduction via spark	25
	Cd	Iron ore, slags	Graphite cup	112

* All applications listed are for Ar-N_2 ICP unless stated otherwise.

Table 14
IONIZATION INTERFERENCES AT OPTIMUM CONDITIONS[a] FOR MULTIPLE-ELEMENT ANALYSIS.[104]

Element	Wavelength (nm)	S/B	Ionization Interference (%)
S I	182.0	1	−5
As I	197.1	2	+10
Zn I	213.8	22	−7
P I	214.9	2	+2
B I	249.7	57	−10
Si I	251.6	12	−5
Pt I	265.9	5	−5
Au I	267.5	19	−6
Al I	308.2	4	−12
Cu I	324.7	40	+4
Ag I	328.0	10	+30
Sn II	189.9	4	−16
Pb II	220.3	3	−25
Ni II	231.6	19	−12
Co II	238.8	32	−13
Ta II	240.0	9	−24
Mn II	257.6	290	−14
Fe II	259.9	48	−15
Mg II	279.5	120	−11
Cr II	283.5	67	−14
Nb II	309.4	25	−11
Ca II	317.9	12	−11
Ti II	337.2	27	−11

[a] The compromise optimum conditions were: 4.7 kW forward power; 23 L/min N_2 outer flow; 17 L/min Ar intermediate flow; 1.5 L/min injector flow; and 7 mm observation height.

ple, the excitation temperature measured at 12 mm above the torch exit was 5000 K. In another study, Abdallah and Mermet[33] reported relatively the same rotational and excitation temperatures at 5 mm above the load coil when N_2^+ and species such as Ar I, Fe I, Ti I, and V II were used as thermometric species. Because the percentage of molecular gas in the injector flow for this study[33] was greater than the value used in the previous work,[32] lower temperatures were measured in the latter work,[33] thus indicating indirectly that the use pure molecular gas injector flow may deteriorate the vaporization-atomization efficiency of Ar-supported ICP discharges. Because a small temperature gradient was observed in the axial channel, no Abel inversion on the temperature measurements was conducted by Mermet and associates.[32,33]

2. ICP Discharges with Alternate Outer Gases

As discussed in Section IV.B, both the net analyte and the background intensities are enhanced when up to 10 to 20% of the outer gas flow of the Ar ICP discharge is replaced with molecular gases. This enhancement may be partially attributed to the increase in plasma temperatures. Thus, Batal et al. reported[17] an increase of 700 K when only 0.3% H_2 was added to the outer gas flow of an Ar plasma operated at 1.3

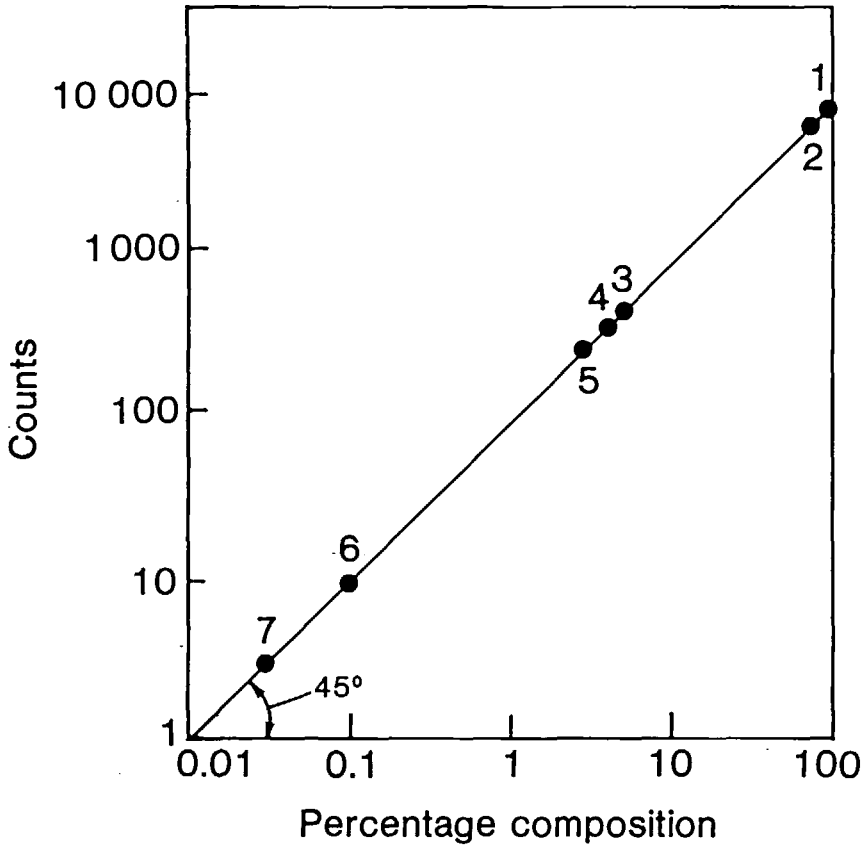

FIGURE 17. Calibration curve obtained for copper in a variety of matrices: (1) BCS 374, phosphor bronze, 89.5% Cu; (2) BCS 264, leaded bronze, 80.5% Cu; (3) BCS 216/2, Duralumin, 4.56% Cu; (4) BCS 181/2, 4% Cu/Al alloy, 3.96% Cu; (5) BCS 300, Al alloy, 1.28% Cu; (6) BCS 263/1, 5% Mg/Al alloy, 0.09% Cu; (7) BCS 262, 10% Mg/Al alloy, 0.03% Cu. (From Greenfield, S., *Proc. Anal. Div. Chem. Soc.*, 13, 279, 1976. With permission.)

kW. In contrast, if the Ar outer flow is totally replaced with a molecular gas, a reduction in temperatures, compared to the Ar ICP discharge, is observed. Houk et al.[15] measured ionization temperatures in the axial channel of a 1.2-kW Ar-N_2 ICP by monitoring Cd^+/I^+ ratios with a mass spectrometer. As shown in Table 16, ionization temperature (T_{ion}) measured at the sampling height of 20 mm above the load coil increased with forward power as a result of larger energy input into the plasma, but T_{ion} declined as higher Ar injector gas flow cooled the axial channel. Ionization temperature for the 1.2-kW Ar-N_2 ICP[15] was at least 1000 K lower than those reported for an Ar ICP.[117] Similar conclusions were achieved when excitation temperatures were measured by the emission method for Ar and Ar-N_2 plasmas generated in a low-gas-flow torch[65] (Table 16).

The R branch lines of N_2^+ were used by Zeeman et al.[44] to measure rotational temperatures in an Ar-air ICP at various observation heights. As shown in Table 16, the maximum rotational temperature (T_{rot} = 8290) was measured at 17 mm above the load coil. Addition of increased amounts of nitrogen to the injector gas shifted maximum T_{rot} to a lower portion in the Ar-air ICP discharge.

From the above discussions, one major conclusion can be drawn regarding temperature measurements in mixed-gas plasmas. Abel-inverted, radial profiles of excitation,

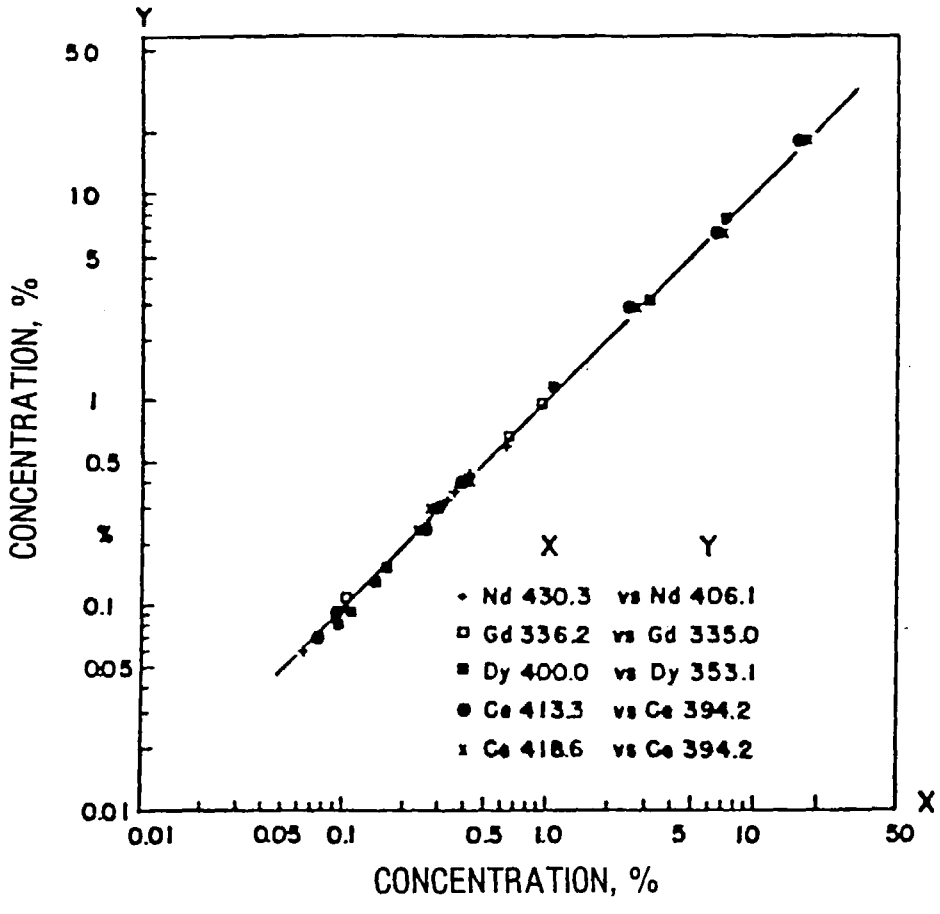

FIGURE 18. Determination of several rare earth elements (Nd, Gd, Dy, Ce) in reference materials using different spectral lines. Sc was used as an internal standard. (From Brenner, I. B., Jones, E. A., and Goncalves, M., *Spectrochim. Acta*, 36B, 785, 1981. With permission.)

rotational, ionization, and electron temperatures must be measured on a single ICP facility before a viable comparison of the data for various mixed-gas plasmas can be made. Only then, the influence of generator frequency, torch design, and detection systems on the data are eliminated. Such measurements may provide evidence of prevailing analyte excitation pathways as a function of location in the ICP, in particular the temperature fields along the axial channel. Relatedly, regions of temperature convergence or regions in which LTE may prevail could be identified.

3. ICP Discharges with Molecular Gases

Kovacic et al.[71] calculated radial excitation and electron temperatures in an air ICP from the measured absolute intensities of 2 atomic nitrogen lines (746.9 and 493.5 nm) and the first negative band of N_2^+ (391.4 nm) for an observation height of −10 to +10 mm referenced to the top of the load coil, Figure 19. These temperature profiles for the air ICP were similar to the radial temperature distributions, obtained experimentally and theoretically, for the nitrogen plasma, Figure 20. In both cases, the radial temperature distribution becomes more uniform above the load coil. The temperature depression along the axial channel, resulting from the injector gas flow, is similar to the behavior observed for the Ar ICP, except that higher temperatures are observed

Table 15
SUMMARY OF TEMPERATURE MEASUREMENTS FOR Ar ICPs WITH MOLECULAR GASES IN THE INJECTOR GAS FLOW[a]

Injector gas flow, ℓ/min (composition)	Intermediate gas flow, ℓ/min of Ar	Outer gas flow, ℓ/min of Ar	Forward power (kW)	Frequency (MHz)	Observation height (mm)	Thermometric species	Temperature (K)[b] T_{rot}	Temperature (K)[b] T_{exc}	Ref.
1.5 (10% CH_4—90% Ar)	7	7—22	6.0[c]	5.4	0—3	C_2		6100	32
					0	Ar I		7000	
					2	Ar I		6200	
					7	Ar I		5800	
					12	Ar I		5000	
1.0 (25% N_2—75% Ar)	12	0	1.3—1.6	40	5[d]	N_2^+		4470	33
						Ar I		5000	
						Fe I		4800	
						Ti I		4770	
						Ti I		4440	
						V II		4850	
						V II		5090	

[a] Blank spaces refer to continuation of operating conditions.
[b] T_{rot} and T_{exc} refer to rotation and excitation temperatures, respectively.
[c] Only generator power is specified.
[d] This observation height[33] is relative to top of coil. All other observation heights[32] are relative to top of torch.

Table 16
SUMMARY OF TEMPERATURE MEASUREMENTS FOR Ar ICPs WITH MOLECULAR GASES IN THE OUTER GAS FLOW[a]

Injector gas flow, l/min (composition)	Intermediate gas flow, l/min Ar	Outer gas flow, l/min (composition)	Forward power (kW)	Frequency (MHz)	Observation height (mm)	Thermometric species	Temperature (K)[b] T_{rot}	Temperature (K)[b] T_{exc}	Temperature (K)[b] T_{ion}	Ref.
1.0 (Ar)	1.5	15 (N_2)	1.2	27	20	Cd^+/I^+			5750—6700	15
2.0 (Ar)			1.2						5100—6100	
1.0 (Ar)			1.5						6500—7800	
1.0 (Ar)	2.5	5—7 (N_2)	1.2	35	9	Fe I		5929		65
					11			5574		
					13			5714		
1.5 (Ar)	16	50 (air)	6—12[c]	9	7	N_2^+	7040			44
					17		8290			
					35		6460			
2.0 (25% N_2—75% Ar)					7		8340			
					17		6570			
					35		6390			
2.5 (40% N_2—60% Ar)					7		8450			
					17		6820			
					35		6340			

[a] Blank spaces refer to continuation of operating conditions.
[b] T_{rot}, T_{exc}, and T_{ion} refer to rotation, excitation, and ionization temperatures, respectively.
[c] Only the generator power is specified.

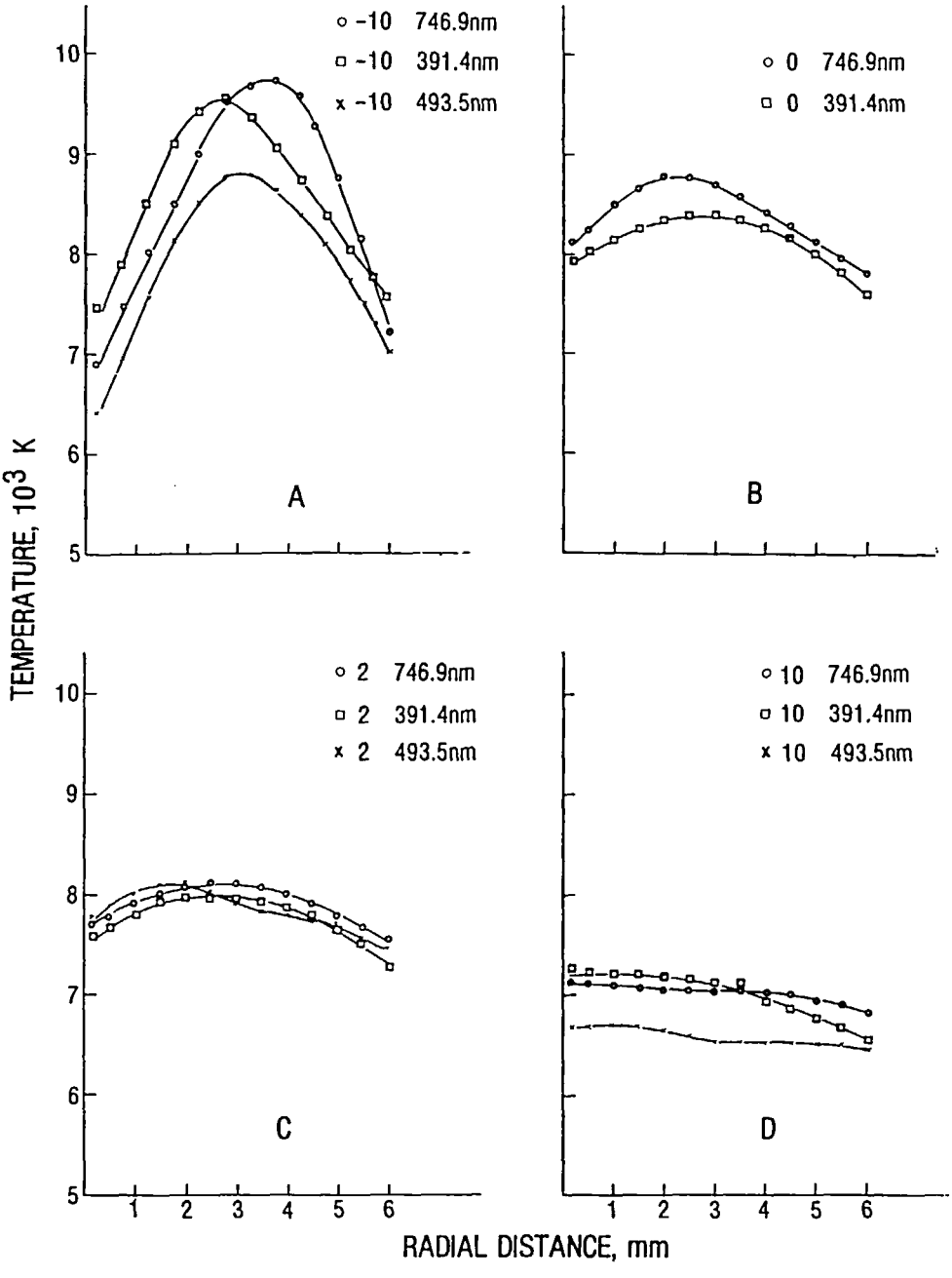

FIGURE 19. Radial excitation temperature distributions in an air ICP at observation heights of (A) −10; (B) ~0; (C) 2; and (D) +10 mm relative to the top of the coil. (From Kovacic, N., Meyer, G. A., Ke-Ling, L., and Barnes, R. M., *Spectrochim. Acta*, 40B, 943 (1985). With permission.)

for the molecular-gas discharges because of the use of higher forward power. One should also note that the temperatures measured at the edges of the molecular-gas plasmas exceed 5000 K, although these plasmas possess smaller apparent volume than Ar ICP discharges, see Section II.A.

For comparison, excitation and electron temperatures extrapolated from the radial temperature profiles[71,118] are listed in Table 17 for both air and nitrogen plasmas. The

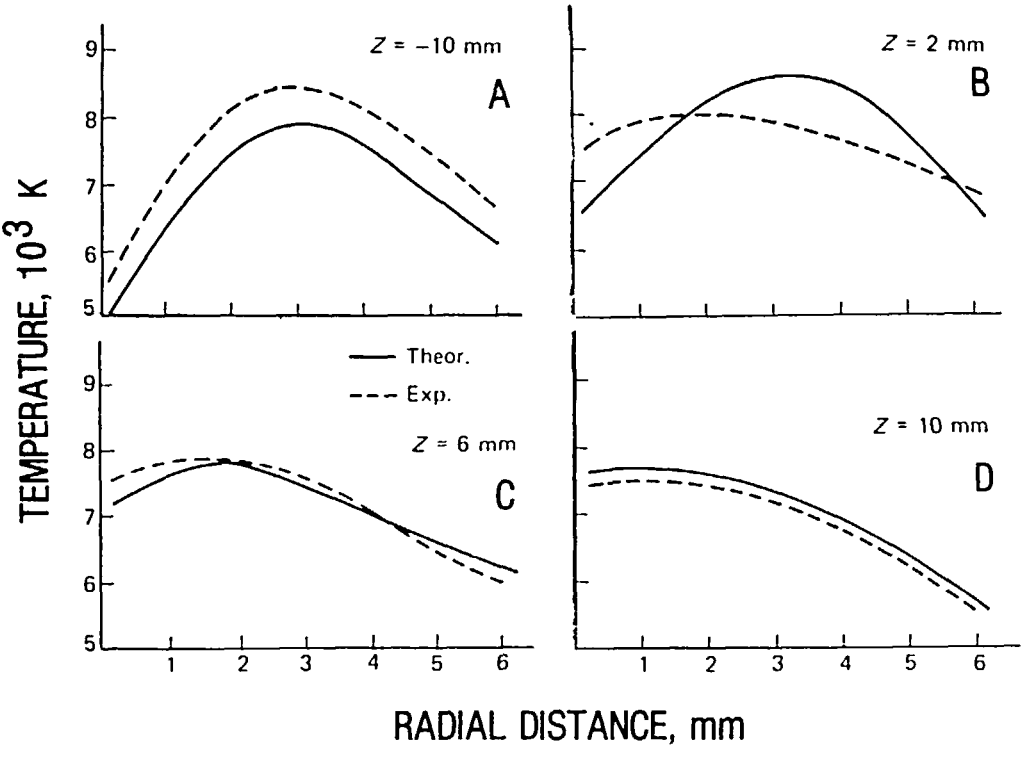

FIGURE 20. Experimental radial temperature profiles in a nitrogen ICP at observation heights of (A) −10; (B) 2; (C) 6; and (D) +10 mm relative to the top of the coil. (From Barnes, R. M., Kovacic, N., and Meyer, G. A., *Spectrochim. Acta*, 40B, 907, 1985. With permission.)

air continuum at 560 nm was used to estimate the electron temperature.[71] Two major conclusions may be drawn from these data. First, the excitation temperatures of air and nitrogen ICPs are roughly the same. Second, although the electron temperature measured in the axial channel is higher than the excitation temperatures at the same location in the air ICP (Table 17), the excellent agreement between the excitation temperatures suggests that the air plasma is closer to LTE than an Ar ICP discharge. The validity of this hypothesis for the N_2 ICP[118] is also supported by the close agreement between theoretical and experimental temperatures obtained for these plasmas. Similar diagnostic studies, recently presented by Barnes and Yang,[72] illustrate that the O_2 ICP is also closer to LTE than the Ar plasma. However, measurement of ionization temperatures for air, nitrogen, and oxygen ICP discharges is needed before a more definite conclusion can be achieved.

4. Helium ICP Discharges

Abdallah and Mermet[73] measured lateral excitation and rotational temperatures in a filament-type He ICP discharge using Fe I and OH, respectively, as thermometric species (Table 18). Because of the disparity between the excitation (4100 K) and rotational (2400 K) temperatures, these investigators concluded[73] that the filament-type He ICP was far from LTE. The lateral excitation temperature (4180 K) measured at 5 mm above the coil in an annular He ICP by Chan and Montaser[75] was comparable to the value measured in the filament-type helium ICP.[73] Chan and Montaser recently reported[77] lateral rotational temperatures in the annular He ICP, but Abel-inverted excitation, rotational, ionization, and electron temperatures have not been obtained for He ICP discharges.

Table 17
AXIAL CHANNEL TEMPERATURES IN MOLECULAR-GAS ICPs

Injector gas flow, *l*/min (composition)	Intermediate gas flow, *l*/min (composition)	Outer gas flow, *l*/min (composition)	Forward[a] power (kW)	Observation height (mm)	Thermometric species	Temperature[b] (K) T_{ex}	Temperature[b] (K) T_e	Ref.
0.8 (air)	1.5 (air)	24 (air)	3.6	0	N I 746 nm	8100		71
				2		7750		
				10		7100		
				2	N I 493 nm	7800		
				10		6700		
				0	N_2^+	7900		
				2		7600		
				10		7250		
				0	Continuum at 560 nm		9000	
				2			8500	
1.0 (N_2)	1.0 (N_2)	20 (N_2)	3.9	2	N I 746 nm	7500		118
				6		7500		
				10		7400		

[a] At 27 MHz.

[b] Extrapolated from radial temperature profiles;[71,118] T_{ex} and T_e refer to excitation and electron temperatures, respectively.

Table 18
SUMMARY OF TEMPERATURE MEASUREMENTS FOR HELIUM ICPs

Injector gas flow (*l*/min)	Intermediate gas flow (*l*/min)	Outer gas flow (*l*/min)	Forward power (kW)	Frequency (MHz)	Observation height (mm)	Thermometric species	Temperature* (K)		Ref.
							T_{rot}	T_{exc}	
0.2	0.2	15 (air-exter-	0.6	50	Within coil	Fe		4100	73,74
		nal)				OH	2400		
1.8	0	55	1.0	27	5	Fe		4180	75

* T_{rot} and T_{exc} refer to rotation and excitation temperatures, respectively.

Table 19
SUMMARY OF MEASURED n_e (cm^{-3}) VALUES USING THE SERIES LIMIT OF Al.[16]

Plasma type	Forward power (W)	Observation height (mm)	Injector gas flow rate (*l*/min of Ar)[a]	n_m	n_e
Ar ICP[b]	400	15	1.0 (PN)	16	$>8.5 \times 10^{13}$
	900	15	1.0 (USN)	13	4×10^{14}
	1000	15	1.0 (PN)	13	$>4 \times 10^{14}$
	1200	15	1.0 (USN)	13	$>4 \times 10^{14}$
	1500	15	1.0 (USN)	12	7×10^{14}
	1800	15	1.0 (USN)	11	1.4×10^{15}
	2000	15	1.0 (PN)	11	1.4×10^{15}
	3000	15	1.0 (PN)	11	$>1.4 \times 10^{15}$
Ar-N_2 ICP[c]	1200—1800	15	1.5 (USN)	16	$>8.5 \times 10^{13}$
	1000	5	2.5 (PN)	16	$>8.5 \times 10^{13}$
	2000	5	2.5 (PN)	14	2.3×10^{14}
	3000	5	2.5 (PN)	13	4×10^{14}
Ar ICP	1200	15	0.5 (USN)	11	1.4×10^{15}
	1200	15	1.0 (USN)	13	$>4 \times 10^{14}$
	1200	15	1.5 (USN)	14	2.3×10^{14}
	1200	15	2.0 (USN)	16	8.5×10^{13}
Ar-N_2 ICP	2000	5	0.5—2.0 (USN)	14	2.3×10^{14}

[a] The sample uptake rate for pneumatic nebulizer (PN) and the ultrasonic nebulizer (USN) were 2 and 3 m*l*/min, respectively.
[b] The outer gas flow rate was 15 to 20 *l*/min of Ar for forward power of 400 to 2000 W and 25 to 30 *l*/min of Ar at higher power. The intermediate gas flow rate was normally zero except for forward power greater than 2000 W when it was about 1.5 *l*/min of Ar.
[c] The outer gas flow were adjusted to 15, 20, and 43 *l*/min of N_2, respectively, for forward powers of 1000 to 1800, 2000, and 3000 W. The intermediate gas flow was 2.5 *l*/min of Ar.

B. Electron Number Density Measurements

1. ICP Discharges with Alternate Injector Gases

Alder and Mermet[32] measured the electron number density (n_e) in Ar and Ar-CH_4 plasmas by monitoring the Stark-broadened H I 486-nm line. The addition of 0.3 *l*/min of CH_4 to the Ar injector gas flow of an Ar ICP decreased n_e from 6.1×10^{15} to $4.9 \times 10^{15} cm^{-3}$. The observation height used in this determination[32] was not reported, however.

Although several investigators have shown[29,57,59,61,62] that addition of molecular gases into the injector flow of Ar ICP deteriorates analytical performance, electron number densities have not been measured in Ar plasmas using other molecular gases in the injector gas. Such studies may provide evidence of reaction mechanisms prevailing in the axial channel of the ICP discharge.

2. ICP Discharges with Alternate Outer Gases

The series-limit-line merging of aluminum was used by Montaser and Fassel[16] to compare n_e values in the axial channel of Ar and Ar-N_2 plasmas. The outer flow of the Ar-N_2 ICP contained pure nitrogen. The influence of forward power, injector gas flow, and observation height on n_e was studied.[16] Electron number densities in the Ar-

N_2 ICP were generally lower than the values obtained for an Ar plasma when the plasmas were compared under similar operating conditions (Table 19). However, comparable n_e values (4×10^{14} cm^3) were obtained when the Ar ICP was operated under commonly used conditions, i.e., 1.2-kW forward power and 15-mm observation, and the Ar-N_2[16,57] was operated at conditions suitable for observation of hard lines, i.e., 3 kW and 5 mm (Table 19). Under the conditions suitable for the observation of soft lines in the Ar-N_2 ICP, 1- to 1.2 kW forward power and 15-mm observation height, the n_e value of the Ar-N_2 plasma was about a factor of five lower than that of Ar ICP discharge operated at the commonly used conditions. The lower n_e values of the Ar-N_2 ICP under the above conditions may partly explain[16,60] the greater susceptibility of the discharge to ionization interferences compared to the Ar plasma.

The electron number densities discussed so far were not Abel inverted. Choot and Horlick[18] obtained radial n_e profiles for Ar, Ar-N_2, and Ar-O_2 plasmas by the Stark broadening method. The n_e maps for Ar and Ar-N_2 ICPs, operated at 2 kW and 1 *l*/min of injector gas flow, are shown in Figure 21. In general, for both Ar-O_2 and Ar-N_2 ICPs, increasing the molecular gas content of the outer flow from 0 to 100% shifted n_e maxima from 15 to 20 mm in Ar plasma to 2 to 5 mm in the mixed-gas plasmas. The highest electron number densities were obtained when Ar-N_2 and Ar-O_2 ICPs contained 10% N_2 or O_2 in the outer gas flow, respectively. The n_e values in these plasmas were about 20 to 30% higher than the largest n_e value in Ar ICP discharge. As discussed before, this increase in n_e values may be correlated with enhancement observed in analyte intensity, background intensities, S/B and S/N ratios.[57,62-64] When the outer flow was totally replaced with N_2 or O_2, the maximum n_e values were pushed towards the axial channel, and the n_e values at the edges of the discharge decreased significantly, reflecting the reduction noted in the size of the discharge.

Because Choot and Horlick[18] have failed to compare the n_e values of their Ar-N_2 ICP discharge to those estimated by Montaser and Fassel,[16] at least one significant difference between the two results should be cited. For the 5-mm observation height centered around the axial channel of the Ar-N_2 ICP operated at 2 kW, Choot and Horlick[18] reported n_e values of 2 to 5×10^{15} cm^{-3}, while Montaser and Fassel[16] measured an $n_e = 2.3 \times 10^{14} cm^{-3}$. Such a difference is puzzling, especially when these results are compared to n_e measurements in Ar ICP operated at 2 kW, 15 mm, and 1 *l*/min of injector gas flow. As shown in Figure 21, the n_e values measured by Choot and Horlick[18] range from 2 to 5×10^{15} cm^{-3} compared to 1.4×10^{15} cm^{-3} reported in Table 19 by Montaser and Fassel.[16] In comparing the above differences, the reader should remember that Choot and Horlick[18] used a relatively low-resolution monochromator for their studies, and the n_e values determined by Montaser and Fassel,[16] through the series-limit-line merging technique, represent estimation based on spatial integration.

3. ICP Discharges with Molecular Gases

Kovacic et al.[71] reported radial n_e profiles, obtained via the Saha equation, at various observation heights for an air plasma by measuring the intensity ratios of Mg II/Mg I and Ca II/Ca I. As the observation height was increased from 0 to 10 mm above the coil, the n_e values decreased[71] for a given radial position (Figure 22). In contrast to the n_e profiles for the Ar ICP discharge (Figure 22), relatively flat n_e profiles are observed for the air plasma. However, the electron number density measured in the axial channel of a 3.6-kW air ICP at 4-mm observation height is approximately the same as the value noted at 15-mm observation height for the 1.1-kW Ar ICP. Similar observations were noted by Meyer[70] when comparing n_e values in Ar, air, and N_2 ICP discharges. Recently, Barnes and Yang[72] presented radial electron number density distributions that also exhibit a relatively flat profile for an O_2 ICP generated at 41 MHz in a conventional torch.

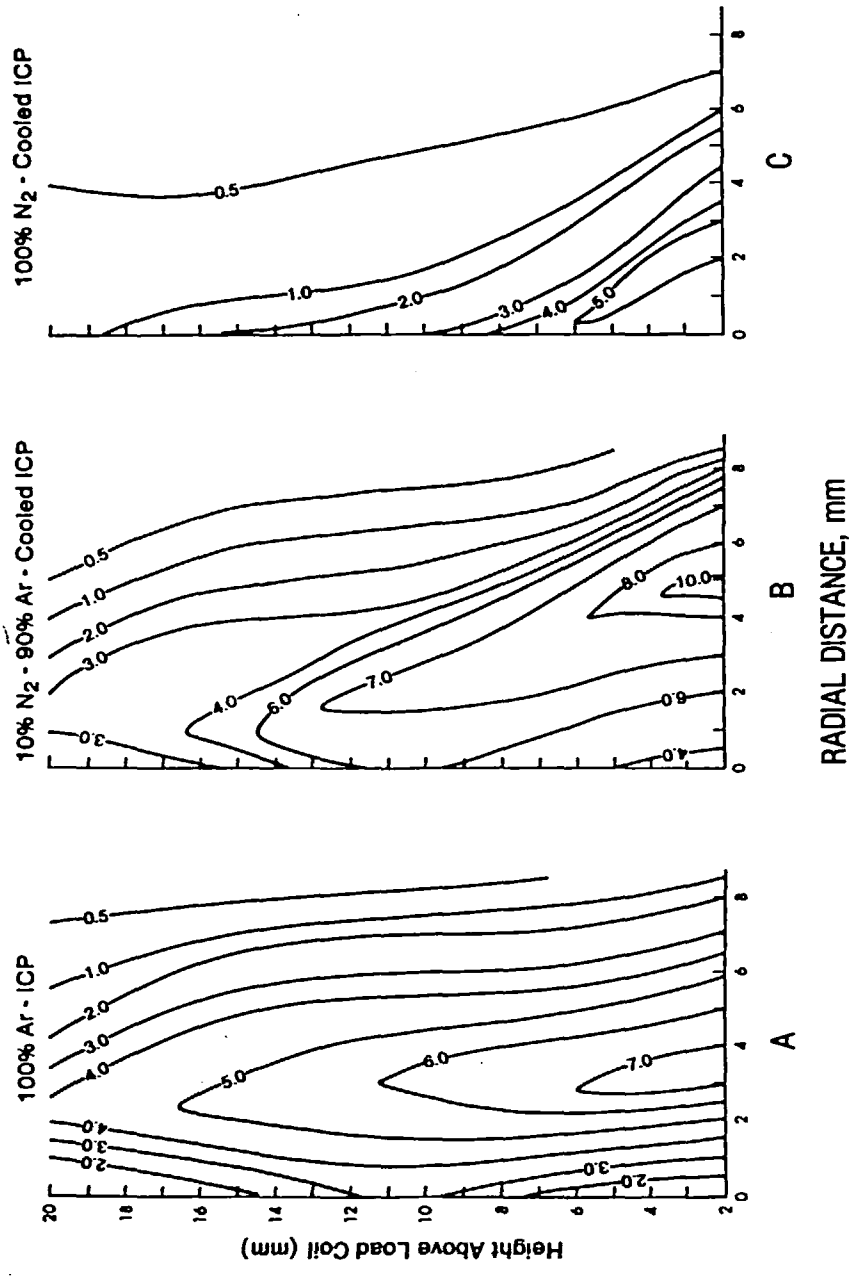

FIGURE 21. The Ne map obtained for Ar, Ar—10% N_2, Ar—100% N_2 ICP discharges. Percentages refer to amount of nitrogen in the other gas flow. (From Chvot, E. H. and Horlick, G., *Spectrochim. Acta*, 41B, 935, 1986. With permission.)

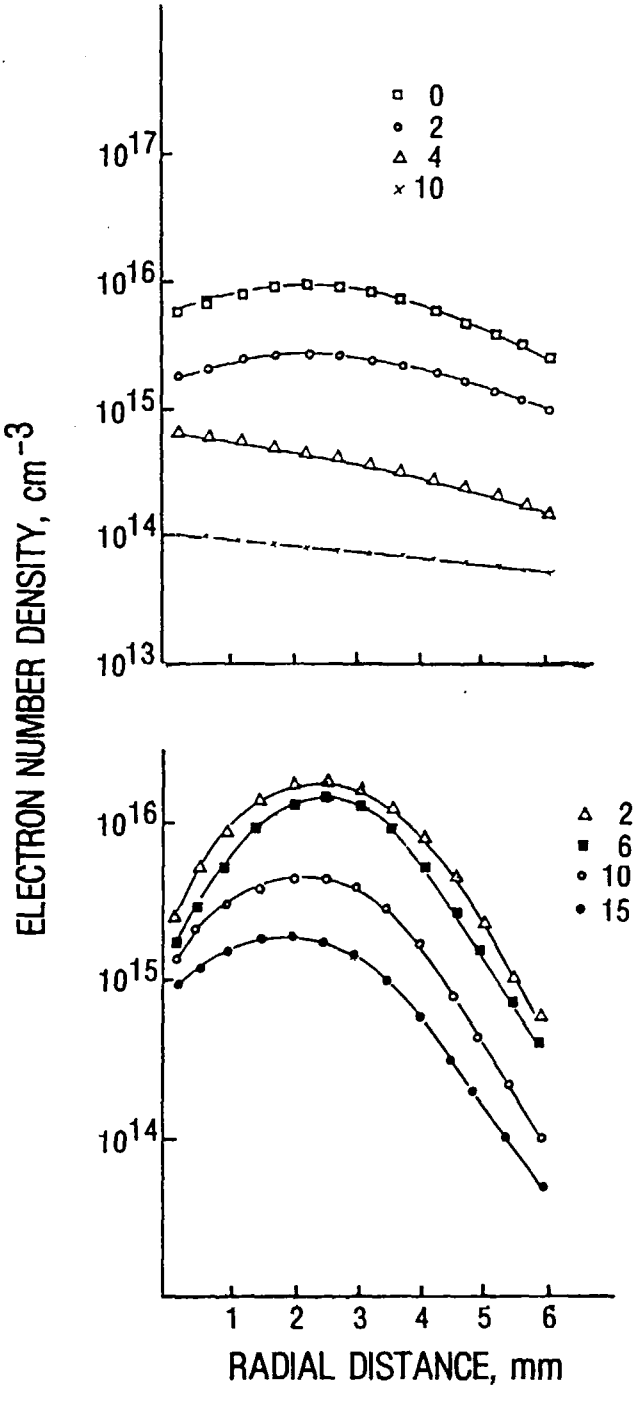

FIGURE 22. Radial distributions of electron number densities at four positions above the load coil for air (top) and Ar (bottom) ICPs based upon ratios of Mg atom and ion intensities. Values in figure refer to observation height relative to top of coil in mm. (From Kovacic, N., Meyer, G. A., Ke-Ling, Liv., and Barnes, R. M., *Spectrochim. Acta*, 40B, 943, 1985. With permission.)

4. Helium ICP Discharges

The electron number density for the annular helium ICP was recently measured by Chan and Montaser[77] using the H_β line. The n_e value, estimated by the least squares method was about $1.7 \times 10^{14} cm^{-3}$ for a He ICP operated at 1.5 kW and 27 MHz.[77]

C. Computer Modeling

Mathematical modeling allows systematic parametric studies of ICP discharges. It predicts profiles for important parameters such as temperature, gas velocity, power input, continuum intensity of the discharge, gas enthalpy, particle decomposition, and magnetic flux density. The various one- and two-dimensional models proposed for ICP discharges have been recently reviewed by Boulos and Barnes.[119] In this section, a brief overview is presented on the applications of the most relevant models to ICP discharges used in spectrochemical analysis. Compared to other nonargon ICP discharges, most modeling studies have focused on molecular-gas plasmas.

Incorporation of realistic gas flows into the two-dimensional model developed by Miller and Ayen[120] enabled Barnes and associates to predict the influence of operating conditions on the spectrochemical behavior of Ar[121-124] and N_2 ICPs.[70,83,84,118,125] Depending on the two-dimensional model used, a set of partial differential equations was solved simultaneously to derive the simulated results. Thus, for example, Barnes and Nikdel[83,84] solved the two-dimensional continuity and energy equations and the one-dimensional electric and magnetic field equation to calculate temperature and flow fields prevailing in ICP discharges. To solve these equations, input data were required on specification of rf generator and torch dimensions, gas flow rates and the velocity distributions, transport properties of the discharge gas as a function of temperature, magnetic flux density distribution, and an initial estimate of temperature distribution. Also, as discussed later, the models were based on several assumptions such as existence of LTE in the ICP discharges.

The most recent model has been described by Mostaghimi et al.[126] For this model, two-dimensional continuity, momentum, and energy equations were solved simultaneously with the one-dimensional electric and magnetic field equation using the SIMPLER algorithm developed by Patankar and Spalding.[127] Compared to other numerical algorithms, improved stability for the model and higher speed of convergence for the solution of the equations were realized with the SIMPLER.[126] So far, this latest model has been used to describe various Ar ICPs,[128-130] a 10-kW N_2 ICP,[128] and a 2-kW O_2 ICP discharge.[72] For these studies, the model was based on the following assumptions: (1) local thermodynamic equilibrium, (2) axially symmetric, two-dimensional temperature and flow fields, (3) one-dimensional magnetic field, (4) steady-state laminar flow, and (5) optically thin plasma.

Computer modeling has led to several theoretical predictions[70,83,84,118] on the physical and spectrochemical properties of molecular-gas ICPs, in particular, for the nitrogen ICP. First, it was predicted[84] that higher forward power was required for forming a N_2 ICP compared to an Ar discharge and that the power distribution profiles peaked closer to the center of the N_2 ICP. Second, radiation energy loss was predicted to be less for the N_2 ICP, while gas enthalpy was expected to be larger than that for an Ar ICP. Third, the use of higher injector gas flow was predicted to have a less significant effect on the temperature of the N_2 ICP compared to the Ar plasma. Fourth, for the same power level, the N_2 ICP was predicted to possess lower temperatures and higher linear gas velocity than an Ar plasma, yet improved particle decomposition rate was anticipated for the N_2 ICP. For example, Barnes and Nikdel[84] estimated that, for a 6.1-kW discharge, the Al_2O_3 particles, with diameters of 25 μm, experience 100% decomposition in a N_2 ICP compared to 40% decomposition in an Ar plasma. It should

be emphasized that laboratory plasmas formed at 27 MHz in Ar and N_2 operate at power levels of 1.5 and 3.5 kW, respectively, and under such conditions, the temperature profiles of a N_2 ICP exhibit larger values than those of an Ar plasma.[118]

Most of the above predictions have been confirmed experimentally. For example, the minimum operating power of a N_2 ICP has been shown to be about 6 times higher than that of Ar discharge operated at 27 MHz.[26,84,118] The fact that direct injection of fine powers into both air and Ar ICPs has resulted in a greater signal from the air ICP[26] indirectly confirms a similar prediction for the N_2 ICP.[84] Barnes et al.[118] also noted reasonable agreement between experimental and theoretical results from the N_2 ICP on properties such as temperature and particle velocity distributions. Close agreement was also reported for the measured and calculated electron number densities in the air ICP.[71] The differences between the experimental and LTE values of intensity ratios of calcium ion-to-atom lines[71] in the air ICP were only within a factor of 3 compared to a factor of 12 to 71 reported for the Ar ICP.[131] These results led Barnes and associates[26,71,118] to conclude that molecular-gas ICPs are closer to LTE than the Ar ICPs. The conclusions have been reconfirmed by recent studies of O_2 ICP discharge,[72] for which the latest model developed by Mostaghimi et al.[126] was used.

Further extensions of modeling studies to air ICP are useful, not only from a fundamental point of view, but because, compared to other molecular-gas discharges, the air ICP has provided the most promising results for elemental analysis, in particular for the determination of air borne particulates and solid samples.[26] Because all previous modeling studies[70,72,83,84,118,120-123,130] of laboratory plasmas did not incorporate magnetic flux density distribution that are obtained experimentally, the need for further improvements of current models seems obvious. Such improvements may not be feasible unless, for example, suitable magnetic probes for measuring magnetic flux density are fabricated that can withstand rf power levels of 0.5 to 4.0 kW. The maximum power level for a recent probe used for an Ar ICP has been limited to 0.6 kW.[70]

Future work on modeling ICP discharges will certainly focus on mixed-gas plasmas and He ICP discharges. We should also note that the accuracy of a model in predicting fundamental parameters of any plasma is closely tied to the ability to measure the same parameters accurately. Thus, future efforts in this area will not only explore improved models, but also improved diagnostic techniques.

VI. CONCLUSIONS AND FUTURE DIRECTIONS

1. Compared to the Ar ICP discharge, higher forward power and higher gas flows are usually required to stabilize and operate both mixed-gas and molecular-gas plasmas. The use of a 41-MHz instead of a 27-MHz generator has significantly reduced the power requirement of the molecular-gas plasmas. The optimum observation height for both mixed-gas and molecular-gas ICPs are usually lower than that of the Ar ICP. However, when pure N_2 is used in the outer flow of Ar-N_2 ICP, soft lines may be optimally observed at 1.2 W and 15 mm, the commonly used conditions for the Ar ICP.
2. Mixed-gas and molecular-gas ICP discharges exhibit a more structured background in the UV region, due to various molecular bands, than the Ar ICP. However, at wavelengths greater than 350 nm, the mixed-gas and molecular-gas plasmas possess a less structured background and, usually, lower continuum background compared to the Ar ICP.
3. With reference to DL, S/N, and S/B ratios, the following conclusions can be achieved when pure molecular gases are used in the outer gas flows of the torch: (1) For an rf power of 4.7 kW, the DLs measured from the Ar-N_2 ICP formed in the Greenfield torch are comparable to those measured from a 1.1-kW Ar ICP

formed in the Fassel torch. (2) For mixed-gas plasmas generated in the Fassel torch, the DL, S/B, and S/N measured at 2.0 kW with the hard lines are inferior by at least a factor of 3 to 5 to those measured from the 1.1-kW Ar ICP. (3) If optimum conditions for the soft lines are used to observe the Ar-N_2 ICP, the DLs are superior or equivalent to those of an Ar ICP discharge.

4. Compared to molecular-gas ICP discharges, the detection limits obtained from the air ICP are superior. A commercial air ICP-atomic emission spectrometer has been introduced into the marketplace for process control application. One should note, however, that the DLs measured for most elements are inferior in air ICP compared to those achieved from the Ar ICP or mixed-gas plasmas, except for the alkali elements. The selection of prominent spectral lines, which remains to be done, may improve the detecting power of molecular-gas ICP discharges. Another area which needs to be investigated, especially if soft lines are to be used for observing the molecular-gas ICP discharges, is the study of matrix interferences.
5. The use of a mixed-gas plasma reduces vaporization-type interferences, although a greater level of ionization-type interference seems to occur, especially at power levels suitable for observing soft lines.
6. Annular He ICP discharges may be formed at atmospheric pressure at 1- to 2-kW forward power. In principle, these plasmas have the potentials to provide the simplest background spectra and the best detection limits for the hard-to-excite spectral lines. These advantages have been documented for the determination of halogens when spectral lines occurring in the red and the near-IR regions are observed. At the present time, however, He ICP discharges exhibit lower temperatures and n_e values than Ar plasmas.
7. Under identical conditions, both the temperature and n_e values of Ar-N_2 ICP, using pure N_2 in the outer flow, are lower than those measured in the Ar ICP. For molecular-gas ICP discharges, the temperature and n_e values measured across the plasma are more uniform than those measured in the Ar plasma. Because molecular-gas ICPs must typically be operated at higher power than the Ar discharge, temperatures reported are also higher. However, relatively the same n_e values have been obtained for a 3.6-kW air ICP and a 1.1-kW Ar ICP.
8. Air, N_2, and O_2 ICP discharges appear to exhibit less departure from LTE than an Ar ICP. Obviously, the suitability of a plasma for spectrochemical analysis does not depend on its attaining LTE. However, computer simulation of N_2 and O_2 ICP discharges has provided relatively good agreement between theoretical results, based on LTE, and the experimental data. Extensions of mathematical modeling to air, mixed-gas, and helium ICP discharges are desirable to facilitate quantitative description of the phenomena which occur in the various discharges. Because most models have assumed LTE to simplify mathematical modeling, future studies should definitely consider the non-LTE phenomenon, especially for He ICP discharges.
9. The major impact of mixed-gas and molecular-gas ICP discharges is their superior ability to decompose refractory particles and to operate with higher solvent and analyte loading compared to Ar ICP, thus extending the domain of samples which could be handled effectively in practice. Because of these properties, direct introduction of solutions and solids into such plasmas must be explored in greater detail. Also, power and gas requirements of molecular-gas discharges must be further reduced so that the Ar ICP users can operate these discharges with their existing facilities. The use of a 100-MHz generator and a low-gas-flow torch should open new opportunities for analytical and fundamental investigations of mixed-gas and molecular-gas ICPs.

10. Although future analytical applications of mixed-gas, molecular-gas, and helium ICP discharges will be concentrated in the emission technique, the unique capabilities of ICP-mass spectrometry, ICP-atomic fluorescence spectrometry, and ICP-atomic absorption spectrometry for diagnostic studies of these plasmas must not be neglected.

ACKNOWLEDGMENTS

This work was sponsored by the U.S. Department of Energy under Contract No. DE-ASO5-84-ER-13172. Acknowledgment is made to the donor of the Petroleum Research Fund, administered by the American Chemical Society, for the partial support of this research. We thank D. W. Golightly of *U.S. Geological Survey* for his helpful comments in revising this article.

REFERENCES

1. Reed, T. B., *J. Appl. Phys.*, 32, 821, 1961.
2. Reed, T. B., *J. Appl. Phys.*, 32, 2534, 1961.
3. Greenfield, S., Jones, I. LI., and Berry, C. T., *Analyst*, 89, 713, 1964.
4. Wendt, R. H. and Fassel, V. A., *Anal. Chem.*, 37, 920, 1965.
5. Fassel, V. A. and Kniseley, R. N., *Anal. Chem.*, 46, 1110A, 1974; Fassel, V. A., *Science*, 202, 183, 1978; Fassel, V. A., *Spectrochim. Acta*, 40B, 1281, 1985.
6. Greenfield, S., Jones, I. LI., McGeachin, H. M., and Smith, P. B., *Anal. Chim. Acta*, 74, 225, 1975; Greenfield, S., McGeachin, H. M., and Smith, P. B., *Talanta*, 23, 1, 1976; Greenfield, S., *ICP Inf. Newsl.*, 1, 3, 1975.
7. Boumans, P. W. J. M. and DeBour, F. J., *Spectrochim. Acta*, 30B, 309, 1975.
8. Barnes, R. M., *Crit. Rev. Anal. Chem.*, 7, 203, 1978.
9. Wendt, R. H. and Fassel, V. A., *Anal. Chem.*, 38, 337, 1966; Greenfield, S., Smith, P. B., Breeze, A., and Chilton, N., *Anal. Chim. Acta*, 41, 385, 1968.
10. Magyar, B. and Aeschbach, F., *Spectrochim. Acta*, 35B, 839, 1980; Gillson, G. and Horlick, G., *Spectrochim. Acta*, 41B, 431, 1986.
11. Mermet, J. M. and Trassy, C., *Spectrochim. Acta*, 36B, 269, 1981.
12. Winge, R. K., Fassel, V. A., Peterson, V. G., and Floyd, M. A., *Appl. Spectrosc.*, 36, 210, 1982.
13. Stubley, E. A. and Horlick, G., *Appl. Spectrosc.*, 38, 162, 1984; Keane, J. M., Brown, D. C., and Fry, R. C., *Anal. Chem.*, 57, 2526, 1985.
14. Montaser, A., Huse, G. R., Wax, R. A., Chan, S., Golightly, D. W., Kane, J. S., and Dorrzapf, A. F., Jr. *Anal. Chem.*, 56, 283, 1984; Rezaaiyaan, R. and Heiftje, G. M., *Anal. Chem.*, 57, 412, 1985.
15. Houk, R. S., Montaser, A., and Fassel, V. A., *Appl. Spectrosc.*, 37, 425, 1983.
16. Montaser, A. and Fassel, V. A., *Appl. Spectrosc.*, 36, 613, 1982.
17. Batal, A., Jarosz, J., and Mermet, J. M., *Spectrochim. Acta*, 37B, 511, 1982.
18. Choot, E. H. and Horlick, G., *Spectrochim. Acta*, 41B, 935, 1986.
19. Goldfarb, V. M. and Goldfarb, H. V., *Spectrochim. Acta*, 40B, 177, 1985.
20. Capitelli, M., Cramarossa, F., Triolo, L., and Molinari, E., *Combustion Flame*, 15, 23, 1970.
21. Borgianni, C., Capitelli, M., Cramarossa, F., Triolo, L., and Molinari, E., *Combustion Flame*, 13, 181, 1969.
22. Capitelli, M., *Ing. Chim. Ital.*, 6, 94, 1970.
23. Dagnall, R. M., Smith, D. J., West, T. S., and Greenfield, S., *Anal. Chim. Acta*, 54, 397, 1971.
24. Chen, Xi and Pfender, E., *Plasma Chem. Plasma Process.*, 2, 185, 1982.
25. Aziz, A., Broekaert, J. A. C., Laqua, K., and Leis, F., *Spectrochim. Acta*, 39B, 1091, 1984.
26. Meyer, G. A. and Barnes, R. M., *Spectrochim. Acta*, 40B, 893, 1985.
27. Meyer, G. A., Analysis of metals in organic solvents by total ICP emission spectroscopy; Meyer, G. A., What to consider when contemplating on-line process control with an inductively coupled plasma emission spectrometer; Klueppel, R. J., Spencer, J. L., and Plankey, F. W., Design of an on-line air plasma spectrometer for process control, papers presented at the 1986 Winter Conf. on Plasma Spectrochemistry, Kailua-Kona, Hawaii.

28. Winge, R. K., Peterson, V. J., and Fassel, V. A., *Appl. Spectrosc.*, 33, 206, 1979.
29. Greenfield, S., Jones, I. L., Berry, C. T., and Bunch, L. G., *Proc. Soc. Anal. Chem.*, 2, 111, 1965.
30. Truitt, D. and Robinson, J. W., *Anal. Chim. Acta*, 49, 401, 1970.
31. Truitt, D. and Robinson, J. W., *Anal. Chim. Acta*, 51, 61, 1970.
32. Alder, J. F. and Mermet, J. M., *Spectrochim. Acta*, 28B, 421, 1973.
33. Abdallah, M. H. and Mermet, J. M., *J. Quant. Spectrosc. Radiat. Transfer*, 19, 83, 1978.
34. Schramel, P., Fisher, R., Wolf, A., and Hasse, S., *ICP Inform. Newsl.*, 6, 401, 1981.
35. Schramel, P. and Li-qiang, Xu, *Fresenius Z. Anal. Chem.*, 319, 229, 1984.
36. Northway, S. J. and Fry, R. C., *Appl. Spectrosc.*, 34, 332, 1980.
37. Northway, S. J. and Fry, R. C., *Appl. Spectrosc.*, 34, 338, 1980.
38. Greenfield, S., *Metron*, 3, 224, 1971.
39. Greenfield, S. and Smith, P. B., *Anal. Chim. Acta*, 59, 341, 1972.
40. Greenfield, S. and McGeachin, H. M., *Anal. Chim. Acta*, 100, 101, 1978.
41. Greenfield, S. and Burns, D. T., *Anal. Chim. Acta*, 113, 205, 1980.
42. Greenfield, S. and Smith, P. B., *Anal. Chim. Acta*, 57, 209, 1971.
43. Brenner, I. B., Watson, A. E., Russell, G. M., and Goncalves, M., *Chem. Geol.*, 28, 321, 1980.
44. Zeeman, P. B., Terblanche, S. P., Visser, K., and Hamm, F. M., *Appl. Spectrosc.*, 32, 572, 1978.
45. Terblanche, S. P., Visser, K., and Zeeman, P. B., *Spectrochim. Acta*, 36B, 293, 1981.
46. Broekaert, J. A. C., Leis, F., and Laqua, K., *Talanta*, 28, 745, 1981.
47. Watson, A. E., *ICP Inform. Newsl.*, 5, 553, 1980.
48. Brenner, I. B., Jones, E. A., Watson, A. E., and Steele, T. W., *Chem. Geol.*, 45, 135, 1984.
49. Brenner, I. B., Watson, A. E., Steele, T. W., Jones, E. A., and Goncalves, M., *Spectrochim. Acta*, 36B, 785, 1981.
50. Ebdon, L., Cave, M. R., and Mowthorpe, D. J., *Anal. Chim. Acta*, 115, 179, 1980; Ebdon, L., Mowthorpe, D. J., and Cave, M. R., *Anal. Chim. Acta*, 115, 171, 1980.
51. Ohls, K., *ICP Inform. Newsl.*, 7, 6, 1981.
52. Sommer, D. and Ohls, K., *Fresenius Z. Anal. Chem.*, 295, 337, 1979.
53. Ohls, K. and Sommer, D., *Fresenius Z. Anal. Chem.*, 296, 241, 1979.
54. Ohls, K. and Loepp, H., *Fresenius Z. Anal Chem.*, 322, 371, 1985.
55. Ohls, K. and Sommer, D., *ICP Inform. Newsl.*, 9, 555, 1984.
56. Ohls, K. and Sommer, D., *ICP Inform. Newsl.*, 4, 532, 1979.
57. Montaser, A., Fassel, V. A., and Zalewski, J., *Appl. Spectrosc.*, 35, 292, 1981.
58. Montaser, A. and Mortazavi, J. M., *Anal. Chem.*, 52, 255, 1980.
59. Zalewski, J., M.S. thesis, Department of Chemistry, Iowa State University, Ames, 1978.
60. Montaser, A., Chan, S., Huse, G. R., Vieira, P. A., and Van Hoven, R. L., *Appl. Spectrosc.*, 40, 473, 1986.
61. Choot, E. H., Ph.D. dissertation, University of Alberta, Alberta, Canada, 1982.
62. Choot, E. H. and Horlick, G., *Spectrochim. Acta*, 41B, 889, 1986.
63. Choot, E. H. and Horlick, G., *Spectrochim. Acta*, 41B, 907, 1986.
64. Choot, E. H. and Horlick, G., *Spectrochim. Acta*, 41B, 925, 1986.
65. ZhiZhuang, He., *Fenxi Huaxue*, 11, 181, 1983.
66. ZhiZhuang, He., *Fenxi Huaxue*, 11, 401, 1983.
67. Barnes, R. M. and Meyer, G. A., *Anal. Chem.*, 52, 1523, 1980.
68. Meyer, G. A. and Thompson, M. D., *Spectrochim. Acta*, 40B, 195, 1985.
69. Meyer, G. A. and Barnes, R. M., U.S. Patent 4,482,246, 1984.
70. Meyer, G. A., Ph.D., dissertation, Department of Chemistry, University of Massachusetts, Amherst, 1982.
71. Kovacic, N., Meyer, G. A., Ke-Ling, Liv., and Barnes, R. M., *Spectrochim. Acta*, 40B, 943, 1985.
72. Barnes, R. M. and Yang, P., Diagnostics in a low power oxygen inductively coupled plasma, paper presented at the 1986 Winter Conf. on Plasma Spectrochemistry, Kailua-Kona, Hawaii.
73. Abdallah, M. H. and Mermet, J. M., *Spectrochim. Acta*, 37B, 391, 1982.
74. Robin, J., *Prog. Anal. At. Spectrosc.*, 5, 79, 1982; Abdallah, M. H., Diemiaszonek, R., Jarosz, J., Mermet, J. M., Robin, J., and Trassy, C., *Anal. Chim. Acta*, 84, 271, 1976.
75. Chan, S. and Montaser, A., *Spectrochim. Acta*, 40B, 1467, 1985.
76. Chan, S., Van Hoven, R., and Montaser, A., *Anal. Chem.*, 58, 2342, 1986.
77. Chan, S. and Montaser, A., Analytical performance of an annular helium inductively coupled plasma generated in a low-gas-flow torch, Paper 970, presented at the 1986 Pittsburgh Conf., Atlantic City, N.J.
78. Jarosz, J. and Mermet, J. M., *J. Quant. Spectrosc. Radiat. Transfer*, 17, 237, 1977.
79. Brown, R. M., Jr. and Fry, R. C., *Anal. Chem.*, 53, 532, 1981.
80. Thorpe, M. L., *NASA Contracters Rep. CR-1143*, 1968.
81. Schramel, P., *Spectrochim. Acta*, 38B, 199, 1983.

82. Alder, J. F., Gunn, A. M., and Kirkbright, G. F., *Anal. Chim. Acta*, 92, 43, 1977.
83. Barnes, R. M. and Nikdel, S., *J. Appl. Phys.*, 47, 3929, 1976.
84. Barnes, R. M. and Nikdel, S., *Appl. Spectrosc.*, 30, 310, 1976.
85. Barnes, R. M. and Nikdel, S., *Appl. Spectrosc.*, 29, 477, 1975.
86. Greenfield, S., *Proc. Anal. Div. Chem. Soc.*, 13, 279, 1976.
87. Greenfield, S., McGeachin, H. M., and Smith, P. B., *Anal. Chim. Acta*, 84, 67, 1976.
88. Watson, A. E. and Russell, G. M., *ICP Inform. Newsl.*, 4, 441, 1979.
89. ZhiZhuang, He., *ICP Inform. Newsl.*, 9, 150, 1983.
90. Russell, G. M. and Watson, A. E., *ICP Inform. Newsl.*, 5, 548, 1980.
91. Greenfield, S., McGeachin, H. M., and Smith, P. B., *ICP Inform. Newsl.*, 2, 167, 1976.
92. Greenfield, S., *ICP Inform. Newsl.*, 1, 3, 1975.
93. Broekaert, J. A. C., Wopenka, B., and Puxbaum, H., *Anal. Chem.*, 54, 2174, 1982.
94. Watson, A. E. and Moore, G. L., *South Afr. J. Chem.*, 37, 81, 1984.
95. Scott, R. H., Fassel, V. A., Kniseley, R. N., and Nixon, D. E., *Anal. Chem.*, 46, 75, 1974.
96. Rezaaiyaan, R., Heiftje, G. M., Anderson, H., Kaiser, H., and Meddings, B., *Appl. Spectrosc.*, 36, 627, 1982.
97. Miller, D. C., Seliskar, C. J., and Davidson, T. M., *Appl. Spectrosc.*, 39, 13, 1985.
98. Seliskar, C. J. and Warner, K. D., *Appl. Spectrosc.*, 39, 181, 1985.
99. Wolnik, K. A., Miller, D. C., Seliskar, C. J., and Frick, F. L., *Appl. Spectrosc.*, 39, 930, 1985.
100. Smith, T. R. and Denton, M. B., *Spectrochim. Acta*, 40B, 1239, 1985.
101. Montaser, A. and Fassel, V. A., *Anal. Chem.*, 48, 1490, 1976.
102. Herzberg, G., *Spectra of Diatomic Molecules*, De Van Nostrand, Princeton, N.J., 1950.
103. Pearse, R. W. B. and Gaydon, A. G., *The Identification of Molecular Spectra*, 4th ed., John Wiley & Sons, New York, 1976.
104. Moore, G. L., Humphries-Cuff, P. J., and Watson, A. E., *Spectrochim. Acta*, 39B, 915, 1984.
105. Boumans, P. W. J. M., *Fresenius Z. Anal. Chem.*, 324, 397, 1986.
106. Morgan, S. L. and Deming, S. N., *Anal. Chim. Acta*, 150, 183, 1983; Deming, S. N. and Parker, L. R., Jr., *CRC Crit. Rev. Anal. Chem.*, 7, 187, 1978.
107. Leary, J. J., Brookes, A. E., Dorrzapf, A. F., and Golightly, D. W., *Appl. Spectrosc.*, 36, 137, 1982.
108. Parker, L. R., Jr., Cave, M. R., and Barnes, R. M., *Anal. Chim. Acta*, 175, 231, 1985.
109. Edwards, T. E. and Horlick, G., *Appl. Spectrosc.*, 31, 536, 1977.
110. Broekaert, J. A. C. and Horman, P. K., *Anal. Chim. Acta*, 124, 421, 1981.
111. Watson, A. E., Russell, G. M., and Balaes, G., *ICP Inform. Newsl.*, 2, 205, 1976.
112. Ohls, K., *Spectrochim Acta*, 39B, 1105, 1984.
113. Sommer, D. and Ohls, K., *GIT Fachz. Lab.*, 26, 1015, 1982.
114. Sommer, D. and Ohls, K., *Labor Praxis*, 598, June 1982.
115. Sommer, D. and Ohls, K., *Fresenius Z. Anal. Chem.*, 306, 372, 1981.
116. Tunstall, M., Berndt, H., Sommer, D., and Ohls, K., *Erzemetal*, 34, 588, 1981.
117. Houk, R. S., Svec, H. J., and Fassel, V. A., *Appl. Spectrosc.*, 35, 380, 1981.
118. Barnes, R. M., Kovacic, N., and Meyer, G. A., *Spectrochim. Acta*, 40B, 907, 1985.
119. Boulos, M. I., *Pure Appl. Chem.*, 57, 1321, 1985; Boulos, M. I. and Barnes, R. M., Plasma modelling and computer simulation, in *ICP Emission Spectrometry*, Vol. 2, Boumans, P. W. J. M., Ed., John Wiley & Sons, New York, chap. 9, in press.
120. Miller, R. C. and Ayen, R. J., *J. Appl. Phys.*, 40, 5260, 1969.
121. Barnes, R. M. and Schleicher, R. G., *Spectrochim. Acta*, 30B, 109, 1975.
122. Genna, J. L., Ph.D. dissertation, Department of Chemistry, University of Massachusetts, Amherst, 1980.
123. Schleicher, R. G. and Barnes, R. M., *Spectrochim. Acta*, 36B, 81, 1981.
124. Schleicher, R. G., Ph.D. dissertation, University of Massachusetts, Amherst, 1979.
125. Nikdel, S., Master's thesis, University of Massachusetts, Amherst, 1976.
126. Mostaghimi, J., Proulx, P., and Boulos, M. I., *Numerical Heat Transfer*, 8, 187, 1985.
127. Patankar, S. V., *Numerical Heat Transfer and Fluid Flow*, McGraw-Hill, New York, 1980.
128. Mostaghimi, J., Proulx, P., and Boulos, M. I., *Plasma Chem. Plasma Process.*, 4, 199, 1984.
129. Proulx, P., Mostaghimi, J., and Boulos, M. I., *Int. J. Heat Mass Transfer*, 28, 1327, 1985.
130. Mostaghimi, J., Proulx, P., Boulos, M. I., and Barnes, R. M., *Spectrochim. Acta*, 40B, 153, 1985.
131. Furita, N. and Horlick, G., *Spectrochim. Acta*, 37B, 53, 1982.